Received: 31 July 2021 | Revised: 4 January 2022 | Accepted: 11 January 2022

DOI: 10.1111/mmi.14880

RESEARCH ARTICLE

WILEY

Type III secretion by *Yersinia pseudotuberculosis* is reliant upon an authentic N-terminal YscX secretor domain

Jyoti M. Gurung[1,2] | **Ayad A. A. Amer**[1,2] | **Shiyun Chen**[3] | **Andreas Diepold**[4] | **Matthew S. Francis**[1,2]

[1]Department of Molecular Biology, Umeå University, Umeå, Sweden

[2]Umeå Centre for Microbial Research (UCMR), Umeå University, Umeå, Sweden

[3]Key Laboratory of Special Pathogens and Biosafety, Wuhan Institute of Virology, Center for Biosafety Mega-Science, Chinese Academy of Sciences, Wuhan, China

[4]Department of Ecophysiology, Max Planck Institute for Terrestrial Microbiology, Marburg, Germany

Correspondence
Matthew S. Francis, Department of Molecular Biology, Umeå University, SE-901 87 Umeå, Sweden.
Email: matthew.francis@umu.se

Funding information
Max-Planck-Gesellschaft; National Natural Science Foundation of China, Grant/Award Number: 31570132; Vetenskapsrådet, Grant/Award Number: 2014-2105 and 2018-02676

Abstract

YscX was discovered as an essential part of the *Yersinia* type III secretion system about 20 years ago. It is required for substrate secretion and is exported itself. Despite this central role, its precise function and mode of action remain unknown. In order to address this knowledge gap, this present study refocused attention on YscX to build on the recent advances in the understanding of YscX function. Our experiments identified an N-terminal secretion domain in YscX promoting its secretion, with the first five codons constituting a minimal signal capable of promoting secretion of the signal less β-lactamase reporter. Replacing the extreme YscX N-terminus with known secretion signals of other Ysc-Yop substrates revealed that the YscX N-terminal segment contains non-redundant information needed for YscX function. Further, both *in cis* deletion of the YscX N-terminus in the virulence plasmid and ectopic expression of epitope-tagged YscX variants again lead to stable YscX production but not type III secretion of Yop effector proteins. Mislocalisation of the needle components, SctI and SctF, accompanied this general defect in Yops secretion. Hence, a coupling exists between YscX secretion permissiveness and the assembly of an operational secretion system.

KEYWORDS
hierarchy, localization, protein–protein interaction, secretion signal, substrate sorting, type III secretion chaperone

1 | INTRODUCTION

Type III secretion systems (T3SSs) produced by assorted Gram-negative bacteria consist of ~20 different proteins that sequentially assemble into a syringe-like device that spans four layers of the cell envelope (the inner membrane, the periplasm, the peptidoglycan layer, and the outer membrane). Once fully assembled, bacteria utilize this structure to inject effector proteins into the eukaryotic host cells. Several of these proteins form two well-characterized, and independently assembled oligomeric ring structures—the outer membrane secretin ring and the inner membrane ring (Blocker et al., 2001; Burghout et al., 2004; Diepold et al., 2010; Kimbrough & Miller, 2000, 2002; Koster et al., 1997; Kubori et al., 2000; Ogino et al., 2006). Additionally, an inner membrane export apparatus and cytosolic sorting complex boast ~10 well-conserved proteins common to all flagella- and non-flagella T3SSs (Butan et al., 2019; Diepold et al., 2011; Fabiani et al., 2017; Johnson et al., 2019; Lara-Tejero et al., 2011; Wagner et al., 2010; Zhang et al., 2017). Their role

may involve substrate recognition, sorting, and energizing for substrate export. A needle appendage spans the membrane rings and extends beyond the bacterial surface (Broz et al., 2007; Marlovits et al., 2006; Wood et al., 2008). These components are listed with universal nomenclature in Supplementary Table S1.

The needle appendage is comprised of "early" substrates that represent the first set of components secreted by a functional T3SS (Zhang et al., 2017), and is the conduit through which unfolded substrates are exported to the outside (Dohlich et al., 2014; Radics et al., 2014). A second set composed of "middle" substrates are secreted and either assemble at the needle tip or sit distal to the needle tip to initiate pore formation in the eukaryotic cell membrane (Mattei et al., 2011; Nauth et al., 2018; Park et al., 2018; Russo et al., 2019). Pore formation is required for the correct delivery into the eukaryotic cell interior of a third set of secreted components—the "late" effector proteins. Hence, substrate secretion might be temporally coordinated according to their individual function; "early" secreted substrates possess functions required first, 'middle' substrates function next, while the "late" secreted substrates are the translocated effectors (Dewoody et al., 2013; Diepold & Wagner, 2014; Osborne & Coombes, 2011).

Three clinically relevant pathogenic *Yersinia* species have served as models to study type III secretion, namely *Y. pestis*, *Y. pseudotuberculosis*, and *Y. enterocolitica*. All three species possess the ability to colonize and establish a disease state in humans. This ability is in part due to all harboring a common virulence plasmid that encodes a highly homologous Ysc (*Yersinia* secretion)—Yop (*Yersinia* outer protein) T3SS (Cornelis et al., 1998). The function of the Ysc-Yop T3SS is to target the cytosol of eukaryotic cells a small but potent effector arsenal. Consequently, *Yersinia* can replicate extracellularly because the internalized effectors modulate phagocytic, apoptotic, and proinflammatory cellular signaling mechanisms (Grabowski et al., 2017; Pha & Navarro, 2016; Philip et al., 2016).

In *Yersinia* Ysc-Yop T3S, there is experimental support for a hierarchical substrate secretion and effector targeting model (Mahdavi et al., 2014; Thorslund et al., 2011). For example, Diepold and colleagues identified that a tripartite complex of YscX–YscY-SctV is involved in the control of "early" substrate export (Diepold et al., 2012). SctV is a core component of all T3SSs and is a relatively fixed inner membrane component of the export apparatus (Diepold et al., 2015). On the other hand, the components YscX and YscY are unique to the Ysc-T3SS phylogenetic clade that is also produced by bacteria including species of *Pseudomonas*, *Aeromonas*, *Photorhabdus*, and *Vibrio* (Gazi et al., 2012; Gurung et al., 2018). YscX is believed to be a T3S substrate chaperoned in the cytoplasm by YscY (Day & Plano, 2000), and both are essential for T3S activity (Day & Plano, 2000; Iriarte & Cornelis, 1999). One or more function(s) of native YscX and YscY appears to be evolutionary optimized to contribute unique and essential information for the physical assembly of the Ysc-Yop T3SS by pathogenic *Yersinia* sp. because related proteins failed to restore T3SS function in *Yersinia* mutants lacking *yscX* and/or *yscY*. This was despite a reciprocal YscX–YscY and a YscX–YscY-SctV interactions between member proteins from different bacteria (Gurung et al., 2018).

The initial discovery of YscX and its important role in Ysc-Yop T3SS activity occurred over 20 years ago (Day & Plano, 2000; Iriarte & Cornelis, 1999). Nonetheless, new functional insight has rarely occurred since these seminal publications. This present study addresses this critical knowledge gap by building on the previous findings of Diepold and colleagues (Diepold et al., 2012). In this regard, we hypothesize that YscX secretion is important for T3SS activity. Indeed, we demonstrate herein that YscX is a true T3SS substrate containing a bona fide secretion recognition signal located at the N-terminus. Moreover, disruption of this N-terminal secretor domain creates a general defect in Ysc-Yop T3S, and an effect of this is improper localization of the needle components SctI and SctF to the bacterial periphery. Altogether, our study provides new insights into the hierarchal targeting and export of early substrates during assembly of the Ysc-Yop T3SS in *Y. pseudotuberculosis*. These findings can be applicable to other bacteria such as species within the *Pseudomonas*, *Aeromonas*, *Photorhabdus*, and *Vibrio* genera that are producing a system belonging to the Ysc-T3SS clade.

2 | RESULTS

2.1 | The N-terminal segment of YscX is an effective T3S export signal

YscX is an apparent early Ysc-Yop T3SS substrate (Day & Plano, 2000; Diepold et al., 2012). However, the secretion signal that mediates its secretion has not been identified. Since T3S export signals of substrates are typically located at the N-terminus (Löwer & Schneider, 2009; McDermott et al., 2011; Wang et al., 2013), we examined if the N-terminal residues of YscX could function as an independent secretion signal to promote the T3S of a β-lactamase reporter. Capitalizing on a reporter system established for studies of the SctB N-terminus (Amer et al., 2011), a series of translational fusions between the 5′ end of *yscX* [including the native Shine-Dalgarno (SD) sequence] and a promoterless *bla* allele lacking a secretion signal were generated. Plasmids were maintained *in trans*, and expression of each fusion was controlled by an IPTG-inducible promoter. We assayed by Western blotting total protein fractions recovered from pelleted bacteria as well as protein secreted to the extracellular medium that was collected from trichloroacetic acid-precipitated bacteria-cleared culture supernatants. Sequences of *yscX* encoding all (FULL) or the first 50, 25, 20, 15, 10 and 5 amino acids were all sufficient to produce generous levels of β-lactamase, a portion of which was secreted (Figure 1a). This secretion was dependent on the presence of a functional T3SS, because an isogenic mutant lacking SctU, an integral T3SS component, failed to secrete these fusions (Figure 1a). Critically, the secretion efficiency peaked at $YscX_{25}$-Bla (circa 25%) and

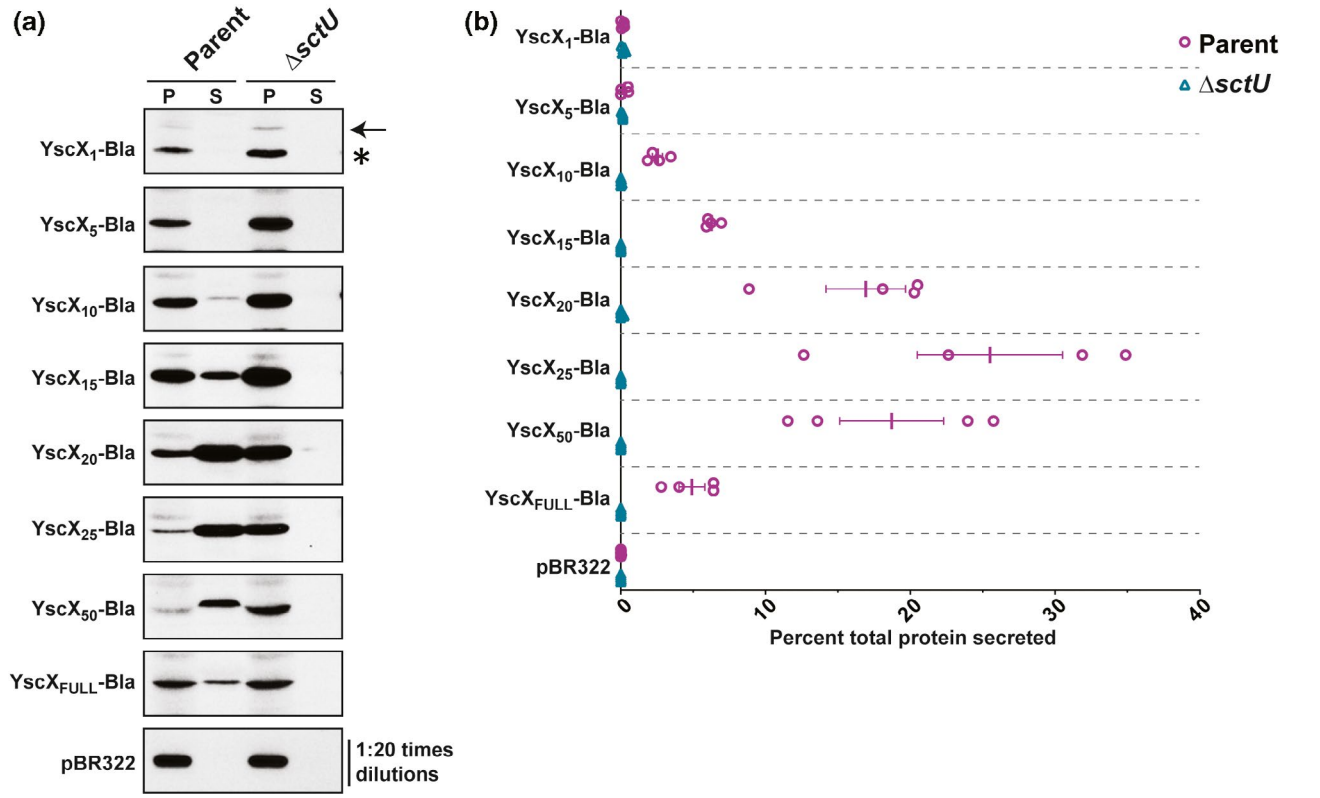

FIGURE 1 T3S of a β-lactamase reporter by appending the YscX N-terminus. Derivatives of pMMB208 contained *yscX-bla* translational fusions placed under control of an IPTG inducible promoter. These constructs were maintained in parental (YPIII/pIB102) and Δ*sctU* null mutant (YPIII/pIB75) bacteria. Overnight cultures of these bacteria were sub-cultured into BHI broth lacking calcium and then grown at 26°C for 1 h and then at 37°C for 3 h. Pellet fractions (P) representing protein associated within intact bacteria and secretion fractions (S) representing protein freely released into the culture supernatant were fractionated by a 12% SDS–PAGE and then transferred onto a membrane support for immune-detection with primary mouse monoclonal anti-β-Lactamase antibody (a). Panels: $YscX_1$-Bla, pJMG010; $YscX_5$-Bla, pJMG012; $YscX_{10}$-Bla, pJMG013; $YscX_{15}$-Bla, pJMG014; $YscX_{20}$-Bla, pAA284; $YscX_{25}$-Bla, pAA285; $YscX_{50}$-Bla, pAA286; $YscX_{FULL}$-Bla, pAA287 and pBR322 (contains native β-lactamase). While the steady-state accumulation of $YscX_1$-Bla (indicated by an arrow) was low in pellet fractions, it could not be detected in secretion fractions. A non-specific cross-reacting band is indicated by an asterisk (*). (b) At least four independent experiments were used to quantify YscX-Bla fusions total production and secretion ± standard errors of the means using Image Lab 6.0.1 (Bio-Rad). Percent total secretion values were calculated as the ratio between the amount of secreted and total protein

descended to $YscX_{10}$-Bla (circa 3%) (Figure 1b). Additionally, $YscX_5$-Bla fusion secretion occurred at an efficiency of <1%, and visualization required overexposure of the immunoblot image (Figure S1a). On the other hand, the smallest *yscX* fusion of 1 amino acids did not visibly promote secretion of the reporter (Figures 1 and S1a). Moreover, we also noted poor steady-state levels of accumulated $YscX_1$-Bla fusion compared to all others (Figure 1a). However, this reduction in accumulation could not be explained by a simple increase in protein turnover, for this smaller fusion was stable (Figure S1b). On the other hand, longer fusions beginning with $YscX_{20}$-Bla were increasingly less stable, and this instability was most dramatic for the largest $YscX_{50}$-Bla and $YscX_{FULL}$-Bla fusions (Figure S1b). This instability would explain the poor secretion efficiency of these larger fusions (Figure 1). Taken altogether, a secretion signal of YscX must minimally consist of 10 or more N-terminal residues. Furthermore, translation efficiency and product stability are two factors that visibly influence the levels of detectable Bla fusions.

2.2 | Deletions within the YscX export signal disrupt its secretion

Given that the N-terminus of YscX is an effective T3S export signal, we wanted to address what impact deleting this region has on YscX synthesis and secretion. Three in-frame deletion mutations in the 5-prime terminus of the *yscX* allele were introduced *in cis* on the virulence plasmid to generate mutant bacteria encoding the variants $YscX_{\Delta 3\text{-}7}$, $YscX_{\Delta 8\text{-}12}$, and $YscX_{\Delta 13\text{-}22}$. To visualize YscX by Western blot, a rabbit polyclonal anti-YscX antiserum was raised against the predicted immunogenic peptide (NH_2-)CLHRAQDYRRELDTL(-$CONH_2$) encompassing the residues 70 to 83 of YscX. Its utility in Western blotting was first checked in protein samples derived from *Yersinia* strains that either lacked YscX or expressed different YscX variants (Figure S2). With this antibody, we first analyzed the susceptibility of each YscX variant to endogenous proteases as an indicator of their ability to form native tertiary folds. Generally, low levels of detectable

accumulated wild type YscX remained similar over time, suggesting it to be stable as long as the cognate T3S chaperone YscY was always present (Figure S3). This corroborates earlier findings of the stabilizing effect of YscY on pre-secretory pools of YscX (Day & Plano, 2000). Critically, there were no obvious differences in stability of accumulated $YscX_{\Delta 3\text{-}7}$, $YscX_{\Delta 8\text{-}12}$, and $YscX_{\Delta 13\text{-}22}$ (Figure S3).

Next, we compared the three YscX mutants to parent bacteria for the ability to secrete YscX during growth in T3S-restrictive (BHI broth plus Ca^{2+} ions) and T3S-permissive conditions (BHI broth minus Ca^{2+} ions). Interestingly, we could only detect the steady-state accumulation of native YscX and very low amounts of $YscX_{\Delta 3\text{-}7}$ associated with the bacterial pellet (Figure 2a, upper panel). Native YscX and $YscX_{\Delta 3\text{-}7}$ were secreted free into the culture medium under

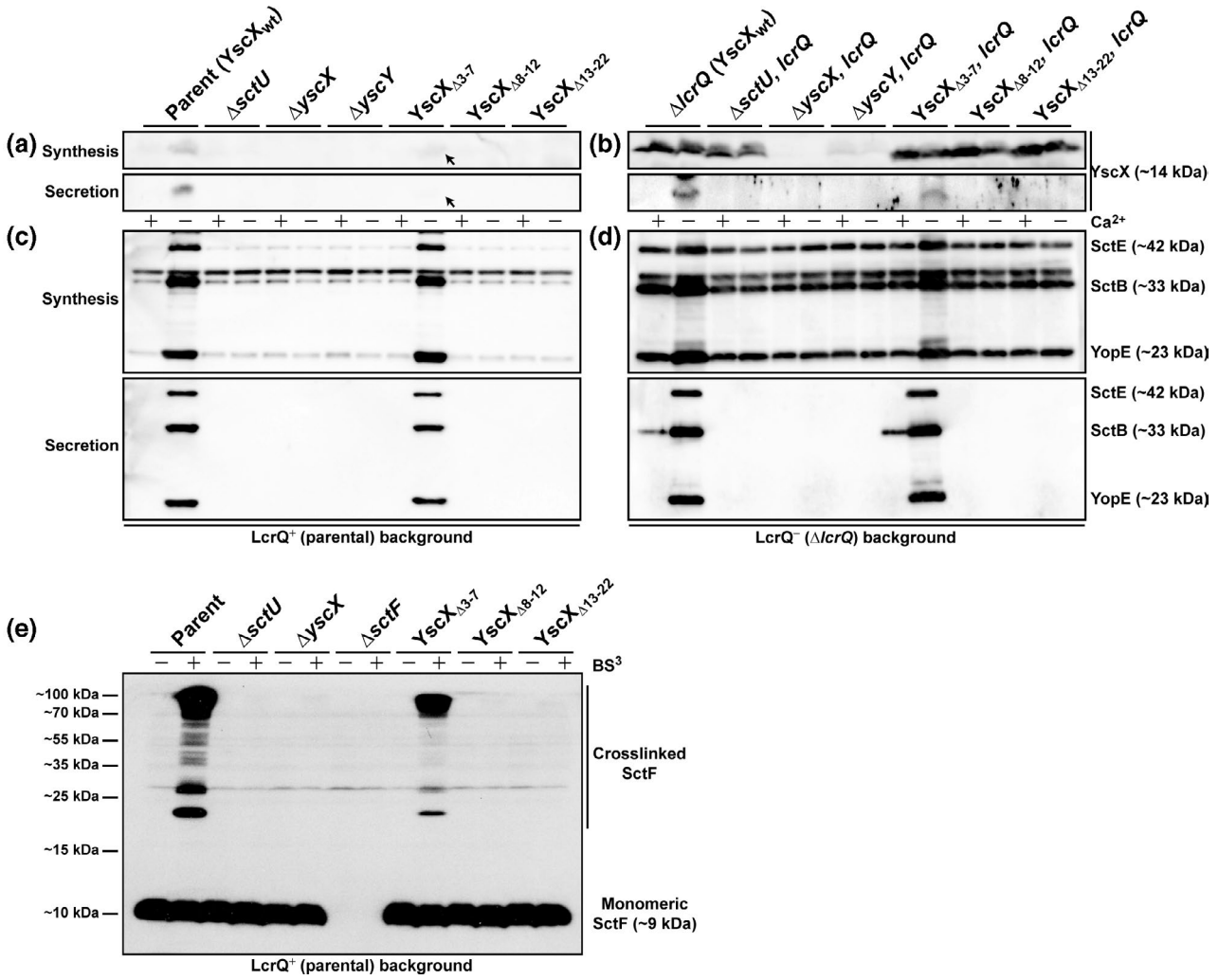

FIGURE 2 Analysis of T3S activity by *Y. pseudotuberculosis* producing YscX variants devoid of N-terminal sequence. Overnight cultures of *Y. pseudotuberculosis* that either harbored an intact *lcrQ* allele (a and c; $LcrQ^+$) or lacked the *lcrQ* allele (b and d; $LcrQ^-$) were sub-cultured into BHI medium in the presence (+) or absence (−) of calcium ions at 26°C for 1 h and at 37°C for 3 h. Protein in the bacterial pellet (Synthesis) and either protein recovered from trichloroacetic acid-precipitated bacterial-free culture supernatant (Secretion—YscX) or protein directly sampled supernatant (Secretion—Yops) were collected and solubilized in sample buffer. Cross-linking of surface localized SctF (E) was performed by growing *Yersinia* strains in non-permissive T3S media (plus Ca^{2+}). Where indicated (+), the membrane-impermeable chemical cross-linker BS^3 was added to the bacteria, subsequently quenched with Tris–HCl and bacteria pellets were solubilized in sample buffer. Protein samples were then fractionated by 15% acrylamide (for YscX and SctF) or 12% acrylamide (for Yops) SDS–PAGE, wet-blotted onto PDVF membrane and then detected using rabbit polyclonal anti-YscX, anti-SctE, anti-SctB, anti-YopE or immune-absorbed monospecific anti-SctF antibodies. Panels A and C: Parental ($YscX_{wt}$), YPIII/pIB102; Δ*sctU*, YPIII/pIB75; Δ*yscX*, YPIII/pIB880; Δ*yscY*, YPIII/pIB890; $yscX_{\Delta 3\text{-}7}$, YPIII/pIB88002; $yscX_{\Delta 8\text{-}12}$, YPIII/pIB88003, $yscX_{\Delta 13\text{-}22}$, YPIII/pIB88004. Lanes B and D: Δ*lcrQ* null mutant ($YscX_{wt}$), YPIII/pIB26; Δ*sctU*, Δ*lcrQ*, YPIII/pIB75-26; Δ*yscX*, Δ*lcrQ*, YPIII/pIB880-26; Δ*yscY*, Δ*lcrQ*, YPIII/pIB890-26; $yscX_{\Delta 3\text{-}7}$, Δ*lcrQ*, YPIII/pIB88002-26; $yscX_{\Delta 8\text{-}12}$, Δ*lcrQ*, YPIII/pIB88003-26, $yscX_{\Delta 13\text{-}22}$, Δ*lcrQ*, YPIII/pIB88004-26. Approximate molecular mass values shown in parentheses were deduced from primary amino acid sequences. The arrow indicates a faint protein band representing $YscX_{\Delta 3\text{-}7}$ that is only clearly visible with prolonged exposure times. Panel E: Parental ($YscX_{wt}$), YPIII/pIB102; Δ*sctU*, YPIII/pIB75; Δ*yscX*, YPIII/pIB880; Δ*sctF* null mutant, YPIII/pIB202; $yscX_{\Delta 3\text{-}7}$, YPIII/pIB88002; $yscX_{\Delta 8\text{-}12}$, YPIII/pIB88003, $yscX_{\Delta 13\text{-}22}$, YPIII/pIB88004. The predicted molecular mass of monomeric SctF is given in parenthesis, while approximate sizes of protein molecular weight standards are given to the left

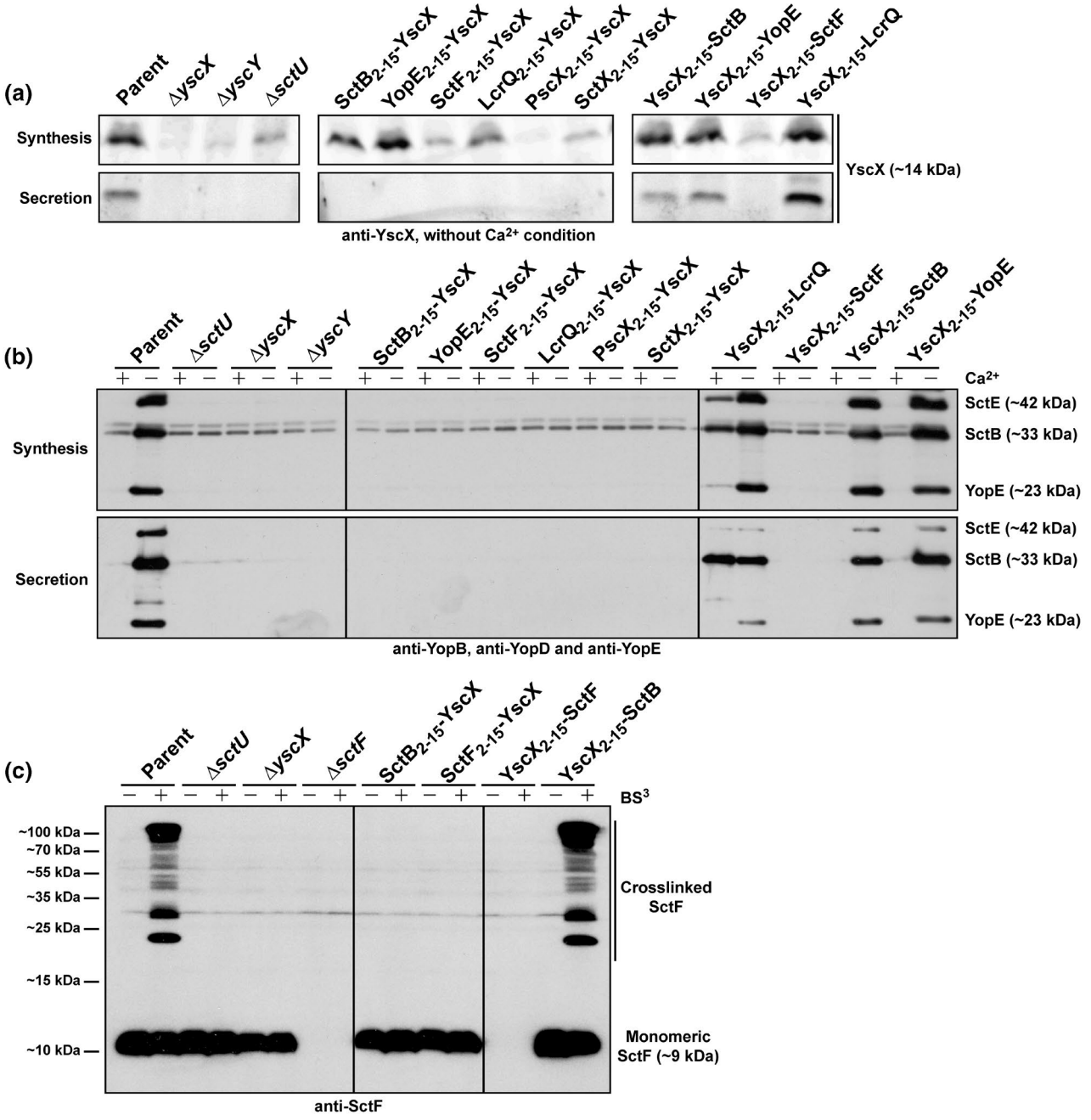

these assay conditions (Figure 2a, lower panel and Figure S2a, lower panel). In the Δ*sctU* null mutant control strain that is T3SS-defective, and in the Δ*yscY* null mutant control strain that is devoid of T3S chaperone activity toward YscX (and is also T3S-defective), production and secretion of YscX were not detectable (Figure 2a).

A dramatic reduction in steady-state levels of $YscX_{\Delta 8\text{-}12}$ and $YscX_{\Delta 13\text{-}22}$ made an analysis of their secretion in isogeneic strains inconclusive. A deletion of *lcrQ*—encoding for a negative regulatory element of Yops synthesis—into the $YscX_{\Delta 3\text{-}7}$, $YscX_{\Delta 8\text{-}12}$, and $YscX_{\Delta 13\text{-}22}$ producing bacteria circumvented this. LcrQ (genetic equivalent YscM1 and YscM2 in *Y. enterocolitica*) is an anti-activator critical to feedback inhibit the Ysc-Yop T3SS. Removal of *lcrQ* leads to de-repression and constitutive production of Yops synthesis even in T3SS-defective bacteria (Li et al., 2014b; Pettersson et al., 1996; Rimpiläinen et al., 1992). Accordingly, analysis of the *lcrQ* mutant for YscX synthesis and secretion displayed a typically de-regulated phenotype, constitutively producing YscX during growth in both non-inductive (BHI plus Ca^{2+} ions) and inductive (BHI minus Ca^{2+} ions) growth conditions, while still only secreting YscX in inductive growth conditions (Figure 2b). Additionally, we could now easily detect YscX synthesis in all strains except for the Δ*yscX* and Δ*yscY* null mutants, yet only parental *Yersinia* as well as the $YscX_{\Delta 3\text{-}7}$ producing strain secreted YscX free into the surrounding medium (Figure 2b). Employing a deletion of *lcrQ* to de-repress Yop synthesis improved the detection of accumulated bacterial-associated pools of YscX variants and confirmed a lack of secretion of $YscX_{\Delta 8\text{-}12}$ and $YscX_{\Delta 13\text{-}22}$, but not of $YscX_{\Delta 3\text{-}7}$. Hence, stably produced YscX is a bona fide T3S substrate of *Y. pseudotuberculosis*, and this secretion

FIGURE 3 Type III secretion activity from bacteria expressing YscX chimeras with a reciprocally exchanged N-terminal secretion signal. Expression and secretion of chimeric substrates with a reciprocally exchanged N-terminal secretion signal. Overnight cultures were sub-cultured into BHI broth lacking calcium and then grown at 26°C for 1 h and then at 37°C for 3 h. Expression and secretion of YscX variants (a) were determined in bacterial pellet (a—upper panel) and TCA precipitated proteins freely released into culture supernatants (a—lower panel) following growth of *Yersinia* in secretion-permissive conditions (-Ca^{2+}). Protein samples were fractionated by a 15% acrylamide SDS–PAGE and then transferred onto a PDVF membrane support for immune-detection with rabbit polyclonal anti-YscX antiserum. Yops (b) associated with total fraction (proteins within intact bacteria and secreted in the culture medium, b—upper panel) and or with supernatant (secreted free to the extracellular medium, b—lower panel) were analyzed following growth of *Yersinia* in BHI medium in the presence (+) or absence (–) of calcium ions. Protein samples were fractionated by a 12% acrylamide SDS–PAGE and then transferred onto a PDVF membrane for immune-detection with rabbit polyclonal antiserum to SctE, SctB and YopE. Surface localized SctF were cross-linked (c) following growth in non-permissive T3S media (plus Ca^{2+}). The membrane-impermeable chemical cross-linker BS^3 was added where indicated (+) and subsequently quenched with Tris–HCl. Bacteria pellets derived protein samples were then fractionated by 15% acrylamide SDS–PAGE, wet-transferred to PVDF and detected with immune-absorbed monospecific anti-SctF antiserum. Synthesis fractions (upper panels) represent bacterial pellet. Secretion fractions (lower panels) signify protein freely released into the culture supernatant. Panel a and b: Parental ($YscX_{wt}$), YPIII/pIB102; Δ*yscX* null mutant, YPIII/pIB880; Δ*yscY* null mutant, YPIII/pIB890; Δ*sctU* null mutant, YPIII/pIB75; $SctB_{2\text{-}15}$-YscX, YPIII/pIB88001; $YopE_{2\text{-}15}$-YscX, YPIII/pIB88007; $SctF_{2\text{-}15}$-YscX, YPIII/pIB88006; $LcrQ_{2\text{-}15}$-YscX, YPIII/pIB88005; $PscX_{2\text{-}15}$-YscX, YPIII/pIB88008; $SctX_{2\text{-}15}$-YscX, YPIII/pIB88009; $YscX_{2\text{-}15}$-SctB, YPIII/pIB62520; $YscX_{2\text{-}15}$-YopE, YPIII/pIB581; $YscX_{2\text{-}15}$-SctF, YPIII/pIB20202; $YscX_{2\text{-}15}$-LcrQ, YPIII/pIB2602. Approximate molecular mass of YscX is shown in parenthesis and was deduced from primary amino acid sequence. Panel c: Parental ($YscX_{wt}$), YPIII/pIB102; Δ*sctU*, YPIII/pIB75; Δ*yscX*, YPIII/pIB880; Δ*sctF* null mutant, $SctB_{2\text{-}15}$-YscX, YPIII/pIB82001; $SctF_{2\text{-}15}$-YscX, YPIII/pIB82006; $YscX_{2\text{-}15}$-SctF, YPIII/pIB20202, $YscX_{2\text{-}15}$-SctB, YPIII/pIB62520. The predicted molecular mass of monomeric SctF is given in parenthesis, while approximate sizes of protein molecular weight standards are given to the left

requires information encoded within its N-terminus, particularly amino acids 8–22.

2.3 | The ability to secrete Yops correlates with YscX secretion

YscX plays a role in promoting T3S (Day & Plano, 2000; Diepold et al., 2012; Iriarte & Cornelis, 1999). We wondered whether YscX secretion is important for this process. Using the strains producing a non-secreted form of YscX *i.e.*: the variants $YscX_{\Delta 8\text{-}12}$ or $YscX_{\Delta 13\text{-}22}$, allowed us to investigate this point. We first used the membrane-impermeable cross-linker BS^3 to examine whether the early substrate—the needle component SctF—could polymerize at the surface of $YscX_{\Delta 3\text{-}7}$-, $YscX_{\Delta 8\text{-}12}$-, and $YscX_{\Delta 13\text{-}22}$-producing bacteria. We detected monomeric SctF located in the bacterial cytoplasm, and therefore protected from the membrane impermeable BS^3 cross-linker, in samples derived from these bacteria as well as in parental bacteria and the T3SS-defective full-length *yscX* and *sctU* deletion mutants (Figure 2e). Only in parental bacteria and $YscX_{\Delta 3\text{-}7}$-producing bacteria, the cross-linking agent BS^3 cross-linked secreted SctF, indicative of higher order structures representative of the T3S needle (Figure 2e). We visualized no cross-linked surface-located SctF in the T3SS-defective full-length *yscX* and *sctU* deletion mutants or in bacteria producing $YscX_{\Delta 8\text{-}12}$ or $YscX_{\Delta 13\text{-}22}$ (Figure 2e). The *sctF* null mutant served as a specificity control to demonstrate that the monospecific anti-SctF antibodies did not cross-react with any other *Yersinia* protein (Figure 2e). Altogether, these data demonstrate that a failure to export $YscX_{\Delta 8\text{-}12}$ or $YscX_{\Delta 13\text{-}22}$ coincided with an inability of these bacteria to assemble a complete T3SS as measured by the absence of a surface appendage composed of polymerized SctF.

We anticipated that strains lacking surface polymerized SctF had abolished T3SS activity. To examine this point, samples derived from $YscX_{\Delta 3\text{-}7}$-, $YscX_{\Delta 8\text{-}12}$-, and $YscX_{\Delta 13\text{-}22}$-producing bacteria were subject to Western blotting to probe for the middle substrates, SctB and SctE, and the late substrate YopE (commonly termed as Yops). As already discussed, *Y. pseudotuberculosis* lacking *yscX*, *yscY, or sctU* are feedback-inhibited for Yops production (Figure 2c) (Bröms et al., 2005; Lavander et al., 2002), but the introduction into these strains of an *lcrQ* deletion to avoid the production of this repressor element restored partial Yops synthesis in both T3S-restrictive (high Ca^{2+}) and T3S-permissive growth media (low Ca^{2+}) (Figure 2d). Not surprisingly, however, these bacteria could not secrete Yops regardless of whether LcrQ was present (Figure 2c) or absent (Figure 2d). Significantly, this LcrQ-dependent Yop synthesis and secretion profile was mirrored in the mutant bacteria producing $YscX_{\Delta 8\text{-}12}$ or $YscX_{\Delta 13\text{-}22.}$ (Figure 2c,d). In contrast, LcrQ+ bacteria producing native YscX or the stable and secreted $YscX_{\Delta 3\text{-}7}$ variant still actively synthesized Yops in a controlled low Ca^{2+}-dependent manner (Figure 2c), and this control was lost upon removal of *lcrQ* (Figure 2d). Critically, these bacteria maintain tight control of this secretion process because it occurred only during growth in T3S-permissive conditions.

These Yop profiles corroborated with the low calcium growth characteristics of these bacteria. Consistent with being repressed for Yop synthesis, the full-length mutations of *sctU*, *yscY*, and *yscX* all resulted in $LcrQ^+$-bacteria exhibiting a calcium independent (CI) growth phenotype, being able to grow at 37°C regardless of the calcium concentration in the growth medium (Figure S4). Similarly, a CI growth phenotype was also observed for $LcrQ^+$-bacteria producing either $YscX_{\Delta 8\text{-}12}$ or $YscX_{\Delta 13\text{-}22}$ that were also unable to synthesize Yops (Figure S4). In contrast, both $LcrQ^+$-parent bacteria and $LcrQ^+$-mutant bacteria producing the stable and secreted $YscX_{\Delta 3\text{-}7}$ variant required calcium for growth at 37°C (Figure S4). Moreover, deletion of the *lcrQ* allele from all strains prompted a temperature sensitive (TS) growth phenotype (Figure S4). This

is consistent with the *lcrQ* deletion effect being epistatic over any mutations that compromise T3SS assembly and that culminate in bacteria constitutively producing Yops regardless of Ca^{2+} concentration.

Taken together, bacteria that produce and secrete $YscX_{\Delta 3\text{-}7}$ still maintain Ysc-Yop T3SS assembly, Yops secretion, and control, whereas these features are lost in bacteria that can produce but not secrete $YscX_{\Delta 8\text{-}12}$ and $YscX_{\Delta 13\text{-}22}$. Hence, the ability to secrete any T3SS substrate (early, middle, and late) correlates with YscX secretion. The data suggest also that the N-terminal YscX secretor domain is involved in dual functions, having roles in both YscX secretion and T3SS assembly. Moreover, the first 3 to 7 residues of the YscX N-terminus are dispensable for both YscX secretion and T3S assembly and activity.

2.4 | T3SS assembly requires an untainted YscX N-terminus

Our N-terminal deletion analysis identified a requirement for the YscX secretor domain in Ysc-Yop T3SS assembly and activity, which corroborates earlier observations that YscX is needed for needle assembly and to orchestrate secretion of 'middle' translocator and 'late' effector substrates (Diepold et al., 2012). To investigate the possibility to uncouple YscX secretion from T3SS assembly, we took advantage of the fact that the reciprocity of secretion signals among the Ysc-Yop T3S substrates is well-known (Amer et al., 2011; Sorg et al., 2007). We created a small series of *in cis*-encoded YscX chimeric variants that have had the native N-terminal codons 2 to 15 exchanged with a variety of functional secretion signals from the early substrates SctF, the chimera was termed ($SctF_{2\text{-}15}$-YscX) and LcrQ ($LcrQ_{2\text{-}15}$-YscX), the middle substrate SctB ($SctB_{2\text{-}15}$-YscX) and the late substrate YopE ($YopE_{2\text{-}15}$-YscX). Additionally, we generated two chimeric YscX substrates that contain codons 2 to 15 derived from the genetically analogous proteins PscX from *Pseudomonas aeruginosa* which is considered a non-secreted substrate ($PscX_{2\text{-}15}$-YscX) (Bröms et al., 2005; Gurung et al., 2018; Yang et al., 2007) and SctX from *Photorhabdus luminescens* ($SctX_{2\text{-}15}$-YscX) (Duchaud et al., 2003; Gurung et al., 2018). As controls, we generated reciprocal chimeric substrates in SctB, YopE, SctF, and LcrQ by substituting the 2–15 N-terminal codons with equivalent N-terminal codons from YscX to generate $YscX_{2\text{-}15}$-SctB, $YscX_{2\text{-}15}$-YopE, $YscX_{2\text{-}15}$-SctF, and $YscX_{2\text{-}15}$-LcrQ respectively. These control strains produce recombinant SctB, YopE, SctF, and LcrQ but allow detection of native YscX.

We grew bacteria in BHI broth in T3S permissive (minus Ca^{2+}) conditions to examine Yops synthesis and secretion of the chimeric substrates. Interestingly, except for $PscX_{2\text{-}15}$-YscX, all chimeric YscX accumulated sufficiently in the cytosol to be specifically detectable by rabbit polyclonal anti-YscX antibodies (Figure 3a, upper panels). An equivalent amount of native YscX was also detected in bacteria producing the reciprocal chimeras of SctB, YopE, SctF, and LcrQ substrates with the N-terminal codons 2 to 15 from the YscX (Figure 3a, upper right panel). Yet, examination of trichloroacetic acid-precipitated bacteria-cleared culture supernatants did not reveal any YscX chimera secretion by *Y. pseudotuberculosis* (Figure 3a, lower panels). This is not a fault of the assay design, since we could detect secretion of reciprocal chimeras $YscX_{2\text{-}15}$-SctB, $YscX_{2\text{-}15}$-LcrQ and $YscX_{2\text{-}15}$-YopE (Figure 3a, lower right panel). Additionally, we could detect secretion of native YscX by parental bacteria, and this was naturally lost in the isogenic T3SS inactive Δ*sctU* null mutant and the T3S chaperone deficient Δ*yscY* null mutant (Figure 3a, lower left panel).

To determine what impact this had on general T3S activity, Yops synthesis and secretion were examined following bacterial growth in both T3S-restrictive (plus Ca^{2+}) and -permissive (minus Ca^{2+}) growth media. Parental bacteria produced and secreted a profile of SctB, SctE, and YopE that was typically dependent upon the depletion of Ca^{2+} ions (Figure 3b). However, none of these three proteins were detected in bacteria producing any of the YscX chimeras in a pattern observed for the T3SS-defective full-length deletion mutants of *yscX* and *yscY* (Day & Plano, 2000; Diepold et al., 2012) and *sctU* (Lavander et al., 2002) (Figure 3b, upper panel). On the other hand, bacteria producing the reciprocal $YscX_{2\text{-}15}$-SctB, $YscX_{2\text{-}15}$-YopE, and $YscX_{2\text{-}15}$-LcrQ chimeras could all produce and secrete SctB, SctE, and YopE (Figure 3b). Bacteria producing $YscX_{2\text{-}15}$-LcrQ were unique, however because Yops secretion was not calcium restricted (Figure 3b, lower right panel). Unsurprisingly, bacteria producing $YscX_{2\text{-}15}$-SctF could not support Yops production and secretion (Figure 3b). In parallel, we also looked for SctF secretion and its ability to polymerize at the bacterial surface to form the needle appendage—the final step in the assembly of an active Ysc-Yop T3SS. In our assay, the non-membrane permeable chemical cross-linker BS^3 supported SctF polymerization. Given the phenocopy existing among all six N-terminal YscX chimera-producing bacteria, we examined SctF polymerization only in the representative bacteria producing $SctB_{2\text{-}15}$-YscX or $SctF_{2\text{-}15}$-YscX. Although we detected monomeric SctF located in the bacterial cytoplasm (and protected from the membrane impermeable BS^3 cross-linker) in bacteria producing $SctB_{2\text{-}15}$-YscX or $SctF_{2\text{-}15}$-YscX cross-linked surface-located SctF was absent (Figure 3c). Hence, inserting a heterologous N-terminal signal sequence was not sufficient to maintain YscX function.

To rule out the possibility that defective SctF surface polymerization and T3SS activity was actually due to the failed secretion ability of the YscX chimeras, we analyzed YscX secretion uncoupled from YscX-dependent T3SS assembly. This analysis was performed using our reporter assay, where we again translationally fused DNA segments encoding the first 25 residues of $SctF_{2\text{-}15}$-YscX, $LcrQ_{2\text{-}15}$-YscX, $SctB_{2\text{-}15}$-YscX, $YopE_{2\text{-}15}$-YscX, $PscX_{2\text{-}15}$-YscX, and $SctX_{2\text{-}15}$-YscX (including the native SD sequence) to the *bla* allele whose expression is controlled by an IPTG-inducible promoter. Except for two variants—$SctF_{2\text{-}15}$-YscX and $PscX_{2\text{-}15}$-YscX—all others produced recombinant β-lactamase in sufficient quantities to allow secretion by parental bacteria to be detected (Figure S5). Once again, deletion of *sctU* encoding a component of the

T3SS completely abrogated this secretion (Figure S5). Levels of the $SctF_{2\text{-}15}$-YscX and $PscX_{2\text{-}15}$-YscX products were simply too low to determine if they could be secreted. Thus, with two exceptions it is apparent that the heterologous secretion signals are active and maintain the ability to support the T3S of recombinant substrates, such as chimeric YscX.

Hence, YscX chimeras that differ from native YscX only at the N-terminus, by virtue of an exchanged type III recognition and secretion signal, abolished any aspect of T3SS export, including SctF surface polymerization (see Figure 3c), the ability to assemble a competent T3SS able to secrete middle and late substrates such as SctB, SctE, and YopE (see Figure 3b). Accordingly, we conclude that some rudimentary aspects of T3S must rely upon non-redundant peptide sequence in the extreme YscX N-terminus. Given the complexity of T3SS biogenesis and function, this aspect is expected to involve protein interactions with this region of YscX.

2.5 | Interplay between YscX and the T3S chaperone YscY

YscY stabilizes YscX, so the YscY-YscX protein complex is obviously important for T3SS activity (Day & Plano, 2000; Iriarte & Cornelis, 1999). Moreover, T3S chaperones often engage with their cognate substrates through a chaperone binding domain that locates immediately adjacent the N-terminal secretion signal (Francis, 2010). Thus, we next investigated if YscX mutants defective in T3SS assembly and function have lost an ability to interact with YscY. In our hands, the yeast two hybrid system has proven useful in demonstrating a YscX–YscY protein–protein interaction (Bröms et al., 2005). We, therefore, generated *GAL4* activation domain (AD) fusions to *yscX* allelic variants in the vector pGADT7. These were co-transformed along with the pGBKT7 derivative containing *yscY* fused to the *GAL4* DNA binding domain (DBD) into the *Saccharomyces cerevisiae* reporter strain AH109 (James et al., 1996). We confirmed the stable production in yeast of all recombinant variants (Figure S6). Next, we judged a protein–protein interaction according to the ability of the host yeast strain to grow on minimal agar medium lacking either adenine or histidine. A *GAL4* AD fusion to wild type YscX and the three *GAL4* AD fusions to $YscX_{\Delta 3\text{-}7}$, $YscX_{\Delta 8\text{-}12}$ and $YscX_{\Delta 13\text{-}22}$ could all still bind to *GAL4* DBD fused to native YscY binding—as measured by yeast growth—although the degree of $YscX_{\Delta 8\text{-}12}$-YscY interaction was comparatively inferior (Table 1 and Figure S7). Regardless, this degree of interaction with chaperone was sufficient to stabilize pre-secretory pools of all three YscX variants (Figure S3). Given that YscX stability depends on YscY (Day & Plano, 2000; Gurung et al., 2018; Iriarte & Cornelis, 1999), these data reflect that the YscX–YscY complex remains intact in the YscX mutants of *Yersinia*.

TABLE 1 Protein–protein interactions in the yeast two-hybrid assay

Yeast two-hybrid constructs			
DNA-binding domain	Activation domain	*HIS3*$^+$	*ADE2*$^+$
pMF433 (YscY$^+$)	pPJE026 (YscX$^+$)	+++	+++
	pMF921 ($YscX_{\Delta 3\text{-}7}{}^+$)	+++	+++
	pMF922 ($YscX_{\Delta 8\text{-}12}{}^+$)	+(+)	+
	pMF923 ($YscX_{\Delta 13\text{-}22}{}^+$)	+++	+++
	pGADT7	–	–
pGBKT7	pMF921 ($YscX_{\Delta 3\text{-}7}{}^+$)	–	–
	pMF922 ($YscX_{\Delta 8\text{-}12}{}^+$)	–	–
	pMF923 ($YscX_{\Delta 13\text{-}22}{}^+$)	–	–

Notes: *HIS3* and *ADE2* are two reporter genes in *S. cerevisiae* AH109 (Clontech Laboratories). *HIS3*$^+$ and *ADE2*$^+$ represents strong growth (+++) to no growth (–) on minimal medium devoid of histidine or adenine, respectively, recorded after day 4. Due to an intrinsic leakiness with the *HIS3* reporter, 4 mM 3-aminotriazole was added to histidine dropout media to suppress false positives (James et al., 1996). Results reflect trends in growth from three independent experiments in which several individual transformants were tested on each occasion.

2.6 | A core element of Ysc-Yop T3SS assembly, SctV, remains a target of defective YscX

Based upon a previous report (Diepold et al., 2012), a tripartite complex forms between YscX–YscY and the integral inner membrane protein SctV, a core component of all T3SSs. This tripartite complex may contribute to establish a competent T3SS by coordinating early substrate secretion (Diepold et al., 2012). Hence, we wondered whether manipulation of the YscX N-terminus violates YscX–YscY binding to SctV. A yeast three-hybrid assay was established to detect this because both YscX and YscY are required simultaneously for complexing with SctV. A soluble variant of SctV containing only amino acid residues 322 through to 704 was cloned into the plasmid pGADT7 creating a fusion to the C-terminus of the GAL4 activation domain. We also cloned a full-length parental *yscY* allele into the MCSI site in the plasmid pBRIDGE creating a fusion with the GAL4 DNA binding domain. In this vector, the *yscX* allelic variants were then cloned under the control of a methionine repressible promoter (MCSII). Tripartite interactions were determined followed by growth on histidine lacking agar media in the presence or absence of methionine or by β-galactosidase measurements after growth in equivalent liquid media replete with histidine. We observed a specific interaction with SctV only in the presence of both YscY and YscX proteins (Table 2 and Figure S8). Every modified YscX variants could still engage with SctV so long as YscY was also present (Table 2 and Figure S8). As determined by interactions in yeast, vivid defects in Ysc-Yop T3S induced by manipulation of the YscX N-terminus is not due to an inability of these mutants to form a tripartite complex with YscY and SctV. Hence, YscX function must involve another critical molecular target.

2.7 | Manipulation of YscX N-terminus affects localization of SctI and SctF

Disruption of the YscX secretor domain caused a general secretion defect. We wanted to understand why this defect occurs. The

TABLE 2 Protein–protein interactions in the yeast three-hybrid assay

Yeast three-hybrid constructs					
Derivative of pBridge			Derivative of pGADT7	Interaction	
Plasmid	Binding domain (MCSI)	MCSII	Activation domain	HIS3	β-Galactosidase activity (*lacZ*$^+$) [fold induction[a]]
pBRIDGE	none	none	pGADT7	–	0.95 ± 0.15
pBRIDGE	none	none	pJMG043 (SctV$_{322\text{-}704}^+$)	–	0.79 ± 0.12
pMF442	YscY$^+$	none	pGADT7	–	0.808 ± 0.17
pMF442	YscY$^+$	none	pJMG043 (SctV$_{322\text{-}704}^+$)	–	0.836 ± 0.13
pJMG070	YscY$^+$	YscX$^+$	pGADT7	–	0.742 ± 0.13
pJMG070	YscY$^+$	YscX$^+$	pJMG043 (SctV$_{322\text{-}704}^+$)	+++	234.8 ± 29.39 [281]
pJMG071	YscY$^+$	SctF$_{2\text{-}15}$YscX$^+$	pJMG043 (SctV$_{322\text{-}704}^+$)	+++	237 ± 37.58 [283]
pJMG072	YscY$^+$	LcrQ$_{2\text{-}15}$YscX$^+$	pJMG043 (SctV$_{322\text{-}704}^+$)	+++	196.6 ± 45.53 [235]
pJMG073	YscY$^+$	SctB$_{2\text{-}15}$YscX$^+$	pJMG043 (SctV$_{322\text{-}704}^+$)	+++	172.8 ± 5.35 [207]
pJMG074	YscY$^+$	YopE$_{2\text{-}15}$YscX$^+$	pJMG043 (SctV$_{322\text{-}704}^+$)	+++	128.8 ± 9.07 [154]
pJMG075	YscY$^+$	PscX$_{2\text{-}15}$YscX$^+$	pJMG043 (SctV$_{322\text{-}704}^+$)	+++	136.2 ± 9.15 [163]
pJMG076	YscY$^+$	SctX$_{2\text{-}15}$YscX$^+$	pJMG043 (SctV$_{322\text{-}704}^+$)	+++	162.2 ± 22.75 [194]
pJMG077	YscY$^+$	YscX$_{\Delta 3\text{-}7}^+$	pJMG043 (SctV$_{322\text{-}704}^+$)	+++	131.8 ± 9.92 [158]
pJMG078	YscY$^+$	YscX$_{\Delta 8\text{-}12}^+$	pJMG043 (SctV$_{322\text{-}704}^+$)	+++	149.4 ± 23.86 [179]
pJMG079	YscY$^+$	YscX$_{\Delta 13\text{-}22}^+$	pJMG043 (SctV$_{322\text{-}704}^+$)	+++	184.6 ± 38.00 [221]

Notes: *lacZ* is a reporter gene in *S. cerevisiae* Y190 and *HIS3* is a reporter genein *S. cerevisiae* HF7c. Activation of these genes imply an interaction between interactive protein partners fused to the binding domain (MCSI on pBRIDGE) and the activation domain on pGADT7. Expression of the gene cloned into multiple cloning site II (MCSII) is expressed in the absence of methionine. β-Galactosidase activity is recorded in Miller units and is the mean of at least five independent measurements from liquid cultures of logarithmic yeast cells. *HIS3*$^+$ represents strong growth (+++) to no growth (–) on minimal medium devoid of histidine and methionine, recorded after day 4. The standard error of the mean was calculated using Excel software (Microsoft Office suite).

[a]The relative increase in β-Galactosidase activity brought about by the methionine-dependent expression of the *yscX* allele from MCSII. Baseline β-Galactosidase activity is taken from yeast harboring the plasmids pMF442 and pJMG043.

assembly of T3S injectisome is hierarchal, such that the deployment of cell-proximal components occurs before the more distal segments. We wondered if the N-terminus of YscX is required for an aspect of this injectisome assembly process. We first performed Western immunoblotting against different components of T3SS contained within standardized total protein samples (a mix of protein associated with bacteria and the culture supernatant) derived from *Y. pseudotuberculosis* expressing YscX$_{\Delta 3\text{–}7}$, YscX$_{\Delta 8\text{–}12}$, and YscX$_{\Delta 13\text{–}22}$. The genetic background contained an *lcrQ* deletion to uncouple *ysc-yop* expression from the feedback inhibitory loop associated with T3SS assembly checkpoint control. This assay allowed a quick appraisal for altered production of any structural T3SS component in the *yscX*, *lcrQ* mutant backgrounds. This necessitated the production of specific antibodies against purified components of the membrane spanning rings (SctC, SctD, and SctJ), the inner membrane export apparatus (SctV and SctU), and the cytoplasmic components (SctK, SctN, and SctO) (Table S1). In the parental strain, bands were detected representing a protein with an apparent molecular mass of ~60 kDa with anti-SctC antibody, ~42 kDa with anti-SctD antibody, ~25 kDa with anti-SctJ antibody, ~70 kDa with anti-SctV antibody, ~25 kDa with anti-SctK, ~45 kDa with anti-SctN antibody, and ~ 19 kDa with anti-SctO antibody (Figure 4a), which is consistent with the observations of others (Blaylock et al., 2006; Gauthier & Finlay, 2003; Koster et al., 1997; Li et al., 2014b; Mukerjea & Ghosh, 2013; Silva-Herzog et al., 2008; Soto et al., 2017). All these bands were absent in the *Y. pseudotuberculosis* YPIII strain lacking the T3SS encoded virulence plasmid, which confirms the antibody specificity (Figure 4a). Importantly, we could not identify any dramatic deviations between these expression profiles and those derived from the N-terminal YscX mutants (Figure 4a).

Since basal body component production in YscX mutants is not affected, we next investigated if these structures are competent for secretion of "early" substrates such as the SctI adapter/washer and SctF needle filament (Torres-Vargas et al., 2019; Zilkenat et al., 2016). The parental and YscX$_{\Delta 3\text{–}7}$ strains produced and secreted comparable amount of SctI and SctF consistent with a functional T3SS (Figure 4b). While secretion of SctF was calcium-dependent, it was interesting to note SctI secretion irrespective of calcium concentration as reported in a previous study (Figure 4b) (Wood et al., 2008). We also observed reduced accumulation of SctI and SctF in mutants lacking YscX and YscY compared to parental *Yersinia* and the mutant producing YscX$_{\Delta 3\text{–}7}$ (Figure 4b). The lower accumulation of SctI and SctF was consistently mimicked by *Yersinia* strains producing YscX$_{\Delta 8\text{–}12}$ and YscX$_{\Delta 13\text{–}22}$. Moreover, this pool of SctI and SctF was

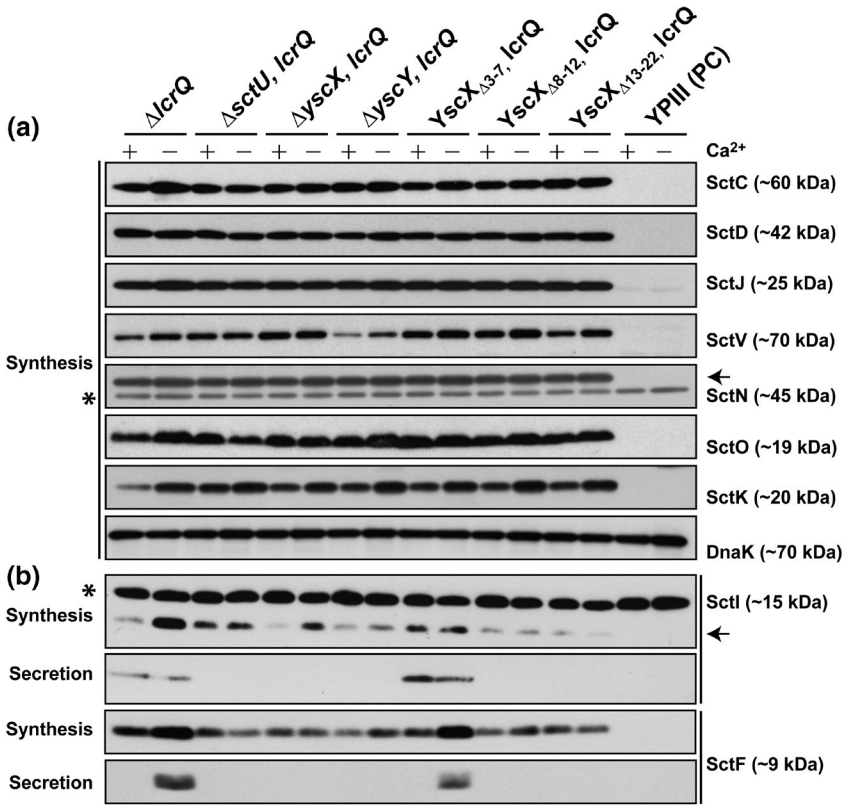

FIGURE 4 YscX influence on the production of Ysc structural components. *Y. pseudotuberculosis* from overnight cultures were sub-cultured into BHI medium in the presence (+) or absence (−) of calcium ions at 26°C for 1 h and at 37°C for 3 h. Protein samples were fractionated by SDS–PAGE in the range of 12 to 18% acrylamide and then transferred onto a PDVF membrane support for immune-detection with rabbit polyclonal antiserum to SctC, SctD, SctJ, SctV, SctN, SctO, SctK and DnaJ (a) as well as to SctI and SctF (b). Synthesis fractions represent bacterial protein (protein within intact bacteria and secreted in the culture medium). Secretion fractions represent protein freely released into the culture supernatant. Strains: Δ*lcrQ* null mutant ($YscX_{wt}$ – parental), YPIII/pIB26; Δ*sctU*, Δ*lcrQ*, YPIII/pIB75-26; Δ*yscX*, Δ*lcrQ*, YPIII/pIB880-26; Δ*yscY*, Δ*lcrQ*, YPIII/pIB890-26; $yscX_{\Delta 3\text{-}7}$, Δ*lcrQ*, YPIII/pIB88002-26; $yscX_{\Delta 8\text{-}12}$, Δ*lcrQ*, YPIII/pIB88003-26; $yscX_{\Delta 13\text{-}22}$, Δ*lcrQ*, YPIII/pIB88004-26; YPIII (PC) is cured of the virulence plasmid. Arrows indicate specific protein band of interest and asterisks identify unknown non-specific cross-reacting proteins. Approximate molecular masses are shown in parenthesis and were deduced from primary amino acid sequence

not secreted (Figure 4b) by the non-functional y*scX* mutants, despite all strains producing equivalent levels of other core structural T3SS components (Figure 4a). This corroborated with the non-secreting control strain lacking SctU (Figure 4b). Hence, a general secretion defect is associated with a specific defect in SctI and SctF synthesis and secretion.

As this might indicate a disordered assembly of the T3SS where one or more individual T3S components exhibit asymmetric distribution in different sub-cellular compartments. To investigate this, sub-cellular localization of different Ysc components was analyzed in fractions derived from the *lcrQ* mutant with intact YscX (parental background) or producing the variants $YscX_{\Delta 3\text{–}7}$ or $YscX_{\Delta 8\text{–}12}$. Analyzed sub-cellular fractions representing the cytoplasm, inner membrane, periplasm and outer membrane fractions were interrogated by Western blotting using our battery of specific antibodies to individual Ysc/Sct proteins. We first confirmed fraction purity using rabbit antibodies to proteins known to be enriched in the outer membrane (OmpA) (Confer & Ayalew, 2013), periplasm (SurA) (Mas et al., 2019), inner membrane (FtsH) (Bittner et al., 2017), and the cytoplasm (H-NS) (Grainger, 2016) (Figure S9). Next, we observed an enrichment of SctC in the outer membrane fractions, SctJ lipoprotein in the periplasmic fraction, and an integral inner membrane protein SctV in the inner membrane fractions (Figure 5a), which corroborated earlier studies (Gauthier & Finlay, 2003; Silva-Herzog et al., 2008). We also detected SctD predominately in the inner membrane fraction (Figure 5a), consistent with it being a component of the inner ring structure (Hu et al., 2017; Lountos et al., 2012). We also observed low levels of all these proteins in the cytoplasmic fraction confirming consistent expression profiles across all strains (Figure 5a). In addition, we observed the cytosolic SctN, SctO, and SctK proteins enriched in the inner membrane fraction (Figure 5a). This is not surprising given their association with integral membrane proteins during their dynamic involvement in active T3SS assembly as shown previously for *Salmonella* (Lara-Tejero et al., 2011). Critically, there was no difference in localization of all these tested components between the parental and the N-terminal YscX mutants. We interpret these data to indicate that assembly of the bacterial envelope spanning "basal body" structure occurs independently of YscX

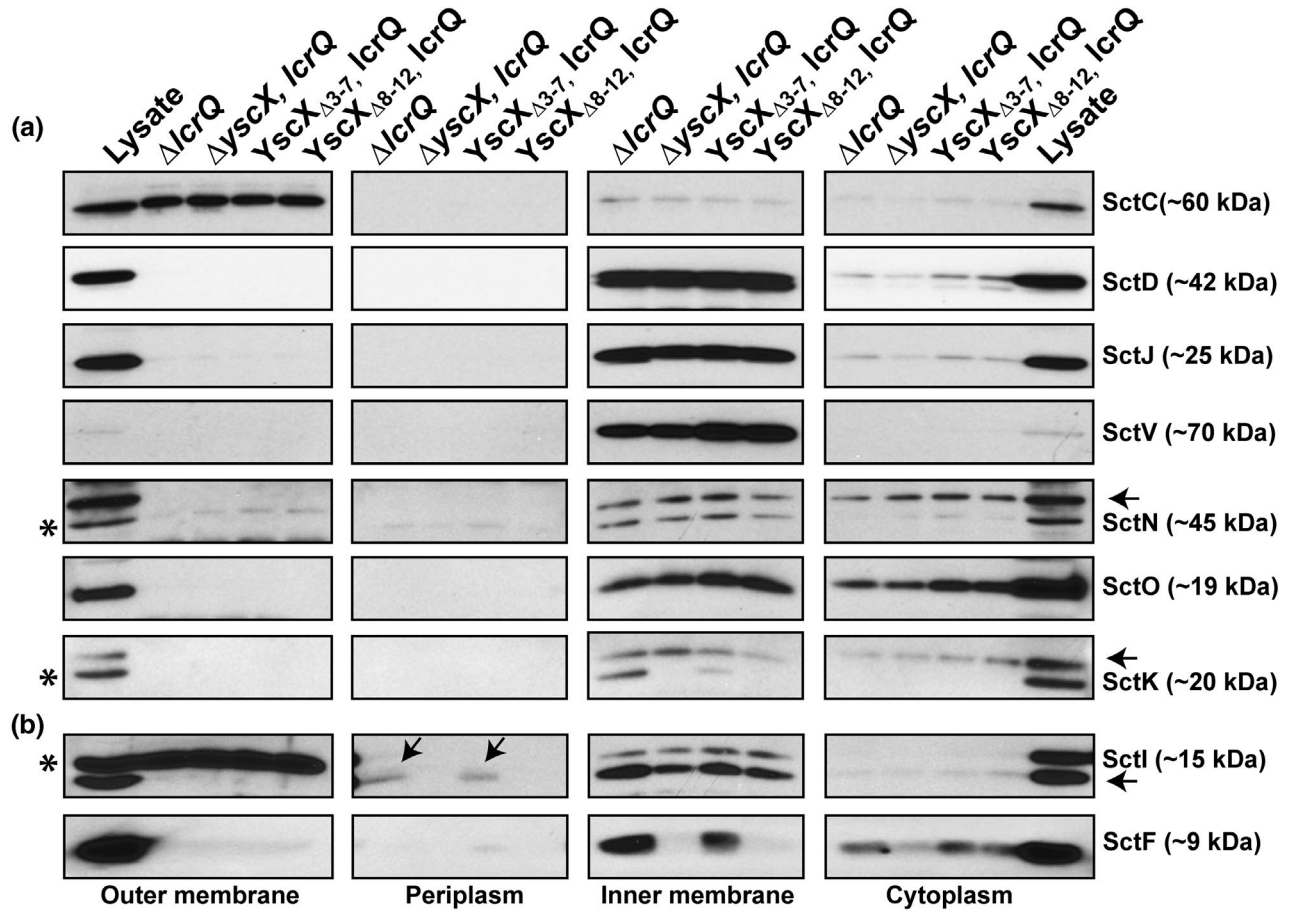

FIGURE 5 Influence of YscX on the spatial localization of Ysc-Yop T3SS components. Sub-cellular fractions representing the cytoplasm, inner membrane, periplasm and outer membrane were prepared from the *lcrQ* mutant with intact YscX (parental background) or producing the variants $YscX_{\Delta 3-7}$ or $YscX_{\Delta 8-12}$. All protein samples were collected from bacteria grown in calcium chelated conditions. The purity of the different cellular fractions was confirmed using rabbit antibodies to OmpA (outer membrane protein marker), SurA (periplasmic protein marker), FtsH (inner membrane protein marker) and H-NS (cytoplasmic protein marker) (Figure S9). Lysate refers to the non-fractionated total cell extract. Samples were analyzed by Western blotting using specific antibodies to SctC (~60 kDa), SctD (~42 kDa), SctJ (~25 kDa), SctV (~70 kDa), SctK (~25 kDa), SctN (~45 kDa) and SctO (~19 kDa) (a), as well as to SctI (~15 kDa) and SctF (~9 kDa) (b). Arrows indicate specific protein band of interest and asterisks identify unknown non-specific cross-reacting proteins. The vertical arrows identify a portion of SctI located to the periplasm. Strains: Δ*lcrQ* null mutant ($YscX_{wt}$), YPIII/pIB26; Δ*yscX*, Δ*lcrQ*, YPIII/pIB880-26; $yscX_{\Delta 3-7}$, Δ*lcrQ*, YPIII/pIB88002-26; $yscX_{\Delta 8-12}$, Δ*lcrQ*, YPIII/pIB88003-26

function. This corroborates earlier findings where SctQ, which itself needs many of the T3SS components for its assembly, was shown to localize perfectly fine in a *yscX* null mutant (Diepold et al., 2010).

We then assessed if the N-terminal YscX deletions affected sub-cellular localization of native SctI and SctF. Strikingly, only parental *Y. pseudotuberculosis* and the $YscX_{\Delta 3-7}$ producing strain could export detectable levels of SctI to the periplasm (Figure 5b). This was despite all strains being capable of targeting SctI for secretion as judged by its widespread presence in the inner membrane fractions (Figure 5b). The absence of SctI in the periplasm of the Δ*yscX* null mutant and bacteria producing $YscX_{\Delta 8-12}$ would indicate an inability to efficiently export and/or assemble SctI at the base of the T3SS needle complex. Given that assembly of the SctI adapter/washer functions as an initiator of SctF needle assembly (Cao et al., 2017; Hu et al., 2018, 2019; Torres-Vargas et al., 2019), we were curious to investigate if SctF assembly is affected under conditions in which the inner rod cannot be completed. Although we observed SctF in the cytosolic fraction in all tested strains, only parental *Y. pseudotuberculosis* and the $YscX_{\Delta 3-7}$ producing strain could export detectable levels of SctF to the inner membrane (Figure 5b). The absence of SctF in the inner membrane fraction of the Δ*yscX* null mutant and bacteria producing $YscX_{\Delta 8-12}$ corroborates observed defects in SctI assembly. These observations suggest that the N-terminal region of YscX is critical for the earliest steps in T3SS export, including the biogenesis of the *Yersinia* T3SS needle complex composed of at least SctI and SctF.

2.8 | Localization of YscX in an active T3SS

Our observations implied that YscX orchestrates ordered export and/or assembly of the early substrates SctI and SctF. We wondered

if defective YscX influenced this role in bacteria containing an intact T3SS. To address this, we first generated the mutant forms of YscX appended with a FLAG™ epitope at the N-terminus. In the low copy number pMMB208 vector, we cloned the alleles under control of an IPTG inducible promoter, before introducing them into parental *Y. pseudotuberculosis*. When induced ectopically with 0.4 mM IPTG, we detected in the synthesis fraction comparable levels of all FLAG-YscX variants (Figure 6a, upper panel). This production did not interfere with the ability of these bacteria to secrete SctB. However, a slight reduction in percent SctE and YopE secretion by bacteria expressing FLAG-$YscX_{\Delta 8-12}$ and FLAG-$YscX_{\Delta 13-22}$ was observed (Figure 6b, lower panel and 6C). Critically, this coincided with a loss of secretion of both FLAG-$YscX_{\Delta 8-12}$ and FLAG-$YscX_{\Delta 13-22}$ by a fully functional T3SS (Figure 6a, lower panel). In contrast, both FLAG-$YscX_{wt}$ and FLAG-$YscX_{\Delta 3-7}$ were efficiently secreted (Figure 6a, lower panel). This corroborated our earlier *in cis* observation (see Figure 2a). Using these same secretion-permissive growth conditions, we performed a sub-cellular fractionation on this strain collection. The ectopically produced FLAG-tagged proteins enriched in the inner membrane fraction, and with a minor amount detected in the cytoplasm fraction (Figure 6d). Inner membrane enrichment of the FLAG-$YscX_{\Delta 8-12}$ and FLAG-$YscX_{\Delta 13-22}$ occurred even though a fully functional T3SS failed to secrete these two proteins (Figure 6a, lower panel). Hence, all three YscX N-terminal variants target the inner membrane, and although not confirmed, presumably meant that all could co-locate to the T3S base, suggesting an interaction with SctV and YscY. However, only FLAG-$YscX_{\Delta 3-7}$ was capable of secretion. Lack of FLAG-$YscX_{\Delta 8-12}$ and FLAG-$YscX_{\Delta 13-22}$ secretion could not be due to interference with SctI and SctF assembly because the export of middle and late T3S substrates continued, albeit at reduced efficiency.

3 | DISCUSSION

Based on the findings in this study, we propose a model that demonstrates the essential need for YscX to establish Ysc-Yop T3SS activity (Figure 7). A consequence of the general secretion defect caused by non-secreted YscX mutants was an inability to correctly localize SctI and SctF and, therefore, a failure to assemble the needle. Hence, the coordinated assembly of the SctI adapter/washer followed by the SctF needle filament indicates that YscX secretion is a key element in mediating spatiotemporal control of early SctI and SctF substrates during Ysc-Yop T3SS assembly.

Our data do not disclose how YscX imparts this control but remains consistent with the suggestion that it is involved in recruitment and sorting of SctI and SctF for prioritized secretion (Wagner et al., 2018). However, the loss of control is not necessarily due to a lack of YscX secretion *per se*. Alternatively, $YscX_{\Delta 8-12}$ and $YscX_{\Delta 13-22}$ may form non-productive interactions with the sorting platform, either because the binding is too tight or because it blocks access points for other substrates. This would result in a general secretion blockage of any substrate, including $YscX_{\Delta 8-12}$ or $YscX_{\Delta 13-22}$ themselves. To investigate these possibilities, we attempted an immunoprecipitation experiment to detect a direct interaction between YscX with either SctI or SctF, which was unsuccessful. However, this negative result is not definitive because the proposed interactions would be transient and initially require formation of the tripartite YscX–YscY-SctV complex, which is an established element of YscX function (Diepold et al., 2011, 2012, 2015).

The fate of secreted YscX remains an enigma. We initially considered that secreted YscX was a minor component of the *Yersinia* T3SS needle following assembly of the basal body, given the role of YscX in SctI and SctF needle biogenesis. However, preliminary results from probing purified needle fractions by Western blot with anti-YscX antisera did not support this hypothesis. Moreover, subcellular localization experiments were also plagued by detection sensitivity issues in immunoblot assays using the anti-YscX antisera. Hence, follow-up efforts to address this enigma must first uncover novel YscX variants that uncouple its roles in needle assembly and general secretion from its own secretion. Then, using these genetic tools combined with a functional fluorescent tagging system, it would be possible to visualize YscX export and targeting at the single cell level with live cell microscopy in real time.

Incidentally, the observation that YscX secretion is a prerequisite for needle biogenesis suggests that YscX may represent a new substrate secretion class secreted prior to the 'early' needle substrates, SctI and SctF. This notion is corroborated by the YscX production and export profile in the $SctU_{(N263A)}$ cleavage site mutant background (Sorg et al., 2007). In this strain, there is some selective enrichment of YscX secretion among the known early-secreted substrates. This prompted us to examine if YscX influenced the SctU auto-cleavage event, a known mechanism of hierarchal secretion control (Bjornfot et al., 2009; Frost et al., 2012; Ho et al., 2017). However, we could demonstrate that SctU auto-cleavage was unaffected by the absence of functional YscX (Figure S10). Thus, despite evidence suggesting that YscX forms a new "pre-early" substrate secretion class, the mechanism orchestrating this secretion order is unclear. Elucidating this mechanism could be difficult because the whole secretion process is unlikely to be linear, even if one would manipulate a population of bacteria to synchronize their secretion.

In this study, we identified YscX as an indispensable component of Ysc-Yop T3SS biogenesis, regulation, and function. Reflecting this essentiality, the YscX amino acid sequence is predominately invariant among 115 fully sequenced strains of *Y. pestis*, *Y. enterocolitica*, and *Y. pseudotuberculosis*. The only exception is observed in a group of 7 sequenced *Y. enterocolitica* strains, where this form of YscX differs by a single Glu to Asp amino acid substitution present at position 28 (BLASTP version 2.10.1+ with the search performed on May 27, 2020) (Altschul et al., 1997, 2005). Hence, YscX function cannot tolerate sequence variation, and this reflects our own genetic complementation studies with both YscX (and YscY) family members that revealed total specificity of YscX (and YscY) for *Y. pseudotuberculosis* T3SS activity (Gurung et al., 2018).

Given the strict coupling of YscX function to the cognate YscY T3S chaperone (Francis, 2010; Pallen et al., 2003), studies aimed

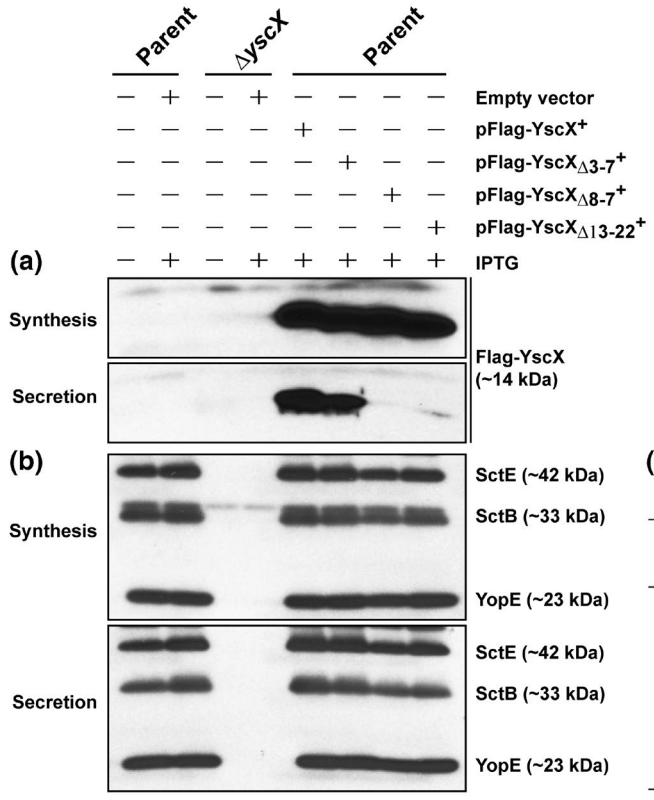

(c)

Strain	Percent total protein secreted		
	SctE	SctB	YopE
Parent	84.2 ± 8.6	73.8 ± 7.8	83 ± 26.5
Parent/Empty vector	85 ± 18.7	68 ± 10.7	71.2 ± 24.1
Parent/pFlag-YscX$^+$	92.8 ± 11.8	89.1 ±10.7	79.4 ± 24.9
Parent/pFlag-YscX$_{\Delta 3\text{-}7}^+$	93.2 ± 11.1	98.1 ± 5.4	71 ± 17.8
Parent/pFlag-YscX$_{\Delta 8\text{-}12}^+$	65.5 ± 28.9	92.8 ± 11.1	59.5 ±17.7
Parent/pFlag-YscX$_{\Delta 13\text{-}22}^+$	74.1 ±27.1	102 ± 19.2	68.1 ± 17.7

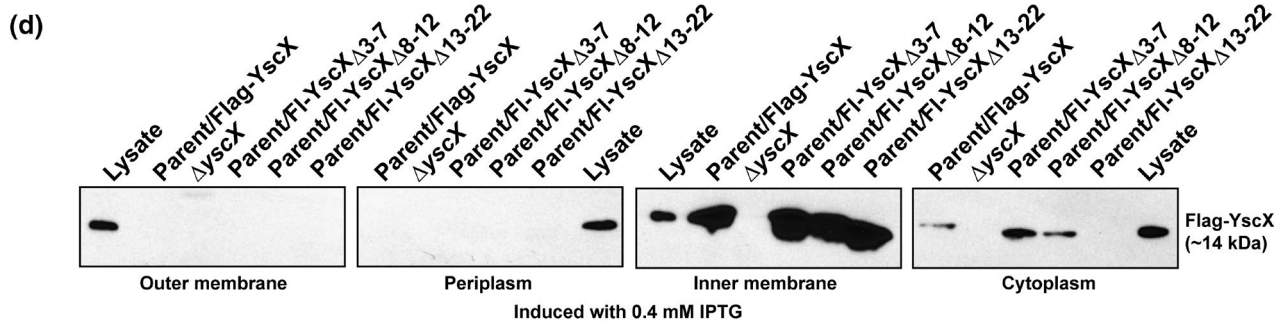

FIGURE 6 Fate of N-terminal FLAG™-tagged YscX variants produced in *Yersinia* with an intact T3SS. Parental bacteria (YPIII/pIB102) were conjugated with vector alone (pMMB208) or vector harboring N-terminal FLAG-tagged *yscX* alleles (FLAG-YscX). Following an overnight culture, *Y. pseudotuberculosis* strains were sub-cultured in BHI broth lacking calcium at 26°C for 1 h and then shifted to 37°C for 3 h. Where indicated, IPTG at a concentration of 0.4 mM was added during the temperature shift. Protein samples from bacterial pellet (Synthesis) and trichloroacetic acid-precipitated bacterial supernatant (Secretion–for YscX variants) or directly sampled supernatant (secretion–Yops) were fractionated by acrylamide SDS–PAGE for recombinant YscX separation (a) or for Yops separation (b). Samples were immunoblotted with mouse anti-FLAG monoclonal antibody (a) or a cocktail of rabbit polyclonal anti-SctE, anti-SctB and anti-YopE antibodies (b). At least three independent experiments were used to quantify relative SctE, SctB and YopE synthesis and secretion values ± standard errors of the means using Image Lab 6.0.1 (Bio-Rad) (c). Percent total secretion values were calculated as the ratio between the amount of secreted and total protein. Sub-cellular fractions representing the cytoplasm, inner membrane, periplasm and outer membrane were prepared from parental bacteria harboring N-terminal FLAG-tagged *yscX* alleles (FLAG-YscX variants) to determine the localization of recombinant YscX variants (d). Lysate refers to the non-fractionated total cell extract. Samples were analyzed by Western blotting using the mouse anti-FLAG monoclonal antibody. Strains: parent (YscX$^+$), YPIII/pIB102; parent/empty vector, YPIII/pIB102, pMMB208; Δ*yscX* null mutant, YPIII/pIB880; Δ*yscX*/empty vector, YPIII/pIB880, pMMB208; parent/FLAG-YscX$_{wt}$, YPIII/pIB102, pJMG242; parent/FLAG-YscX$_{\Delta 3\text{-}7}$, YPIII/pIB102, pJMG349; parent/FLAG-YscX$_{\Delta 8\text{-}12}$, YPIII/pIB102, pJMG350; parent/FLAG-YscX$_{\Delta 13\text{-}22}$, YPIII/pIB102, pJMG352. Approximate molecular mass values shown in parentheses were deduced from primary amino acid sequences

to pry apart YscX–YscY interdependence will shed light on a potential new class of T3S chaperones. Furthermore, interactions between YscX, YscY, and SctV are sequential with the formation of YscX–YscY binding needed for interactions with SctV to occur (Diepold et al., 2012). This indicates that SctV engagement would need conformational changes in YscX and YscY. Advances in this

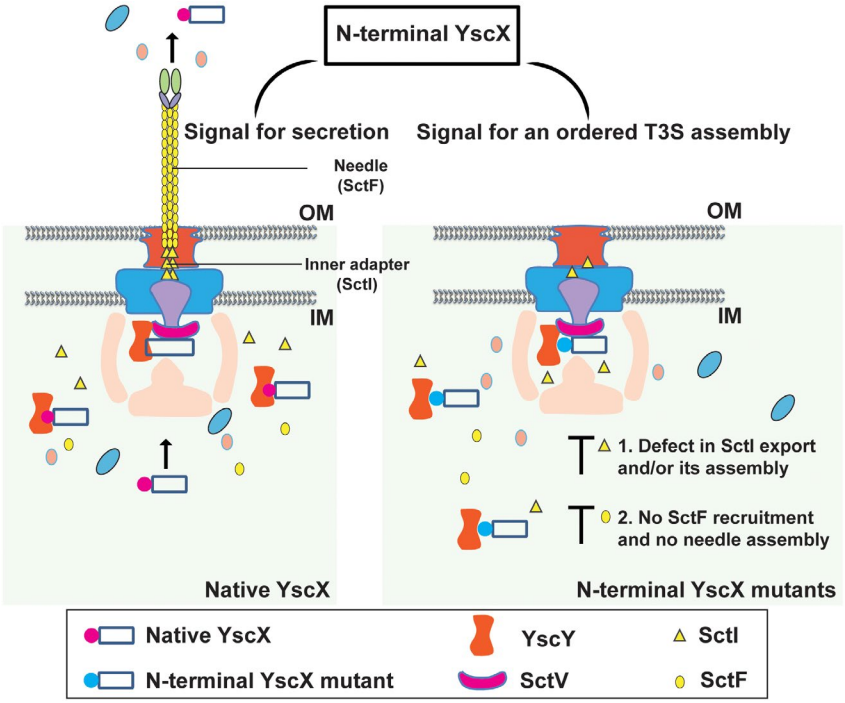

FIGURE 7 Schematic representation of YscX N-terminus mediated control of the Ysc-Yop T3SS. The N-terminal region of YscX (magenta circle) harbors an independent secretion signal that promotes its T3S-dependent secretion. Manipulation of this N-terminal region (blue circle) either by targeted deletion or by defined domain swapping with equivalent secretion signals from other T3S substrates completely disrupts T3SS activity. However, all N-terminal YscX variants maintain an equivalent bipartite interaction with YscY and/or a tripartite interaction with YscY and SctV. Moreover, they are recruited to the inner membrane base in an unbiased manner. The N-terminal region of YscX harbors an additional and a specific recognition signal critical for export and/or assembly of early substrates SctI and SctF. Inset—colored shapes used to depict YscX variants, YscY, SctV, SctI and SctF. IM—inner membrane, OM—outer membrane

process would catalyze opportunities to dissect how this tripartite complex may recognize and prepare the needle components for export, a process that must also involve YscX release from the complex and subsequent export from the bacteria. To this end, the non-secreted mutant forms of YscX described in this study will be helpful in dissecting tripartite complex function in the context of Ysc-Yop T3SS activity, and will also contribute valuable knowledge to elucidate the YscX secretion enigma.

The nature of T3SS injectisomes is generally quite diverse. Therefore, a relevant question concerns how broadly applicable YscX is to all such T3SSs. It is clear from our previous work that YscX is unique to the Ysc-T3SS clade that is produced by certain bacterial species within the *Yersinia*, *Pseudomonas*, *Aeromonas*, *Photorhabdus*, and *Vibrio* genera (Gurung et al., 2018). YscX–YscY heterodimer formation is conserved in this clade, as is an YscX–YscY complex formed with SctV (Gurung et al., 2018), which together mediates export and/or assembly of early T3S substrates (Diepold et al., 2012). In the non-Ysc-T3SS clades that all lack YscX and YscY homologs, the equivalent SctV protein does not appear to possess any additional domains that could accommodate the functions of YscX. This is corroborated by the fact that SctV from *Y. pseudotuberculosis* and *S. enterica*—Typhimurium are not interchangeable (Ginocchio & Galán, 1995). Thus, it is utterly intriguing that the Ysc-T3SS clade has evolved a unique system in YscX–YscY-SctV for coordinating early substrate secretion. Several structural studies have proposed a conserved region in the cytoplasmic domain of SctV that is thought to recognize a chaperone-substrate complex and prepare substrates for secretion (Erhardt et al., 2017; Kuhlen et al., 2021; Majewski et al., 2020; Matthews-Palmer et al., 2021; Xing et al., 2018; Yuan et al., 2021). Hence, SctV has a conserved universal role in all T3SSs, although bacteria producing the Ysc-T3SS clade seems to have customized this function in a way that relies on the YscX–YscY complex. What was the force driving the evolution of this YscX–YscY-SctV connection remains a key question. Nevertheless, in light of a newly discovered accessory protein secreted by the *Salmonella* SPI-1 T3SS that controls needle filament assembly (Kato et al., 2018), or a novel chaperone-mediated secretion switching from early to middle substrates in the *Salmonella* SPI-2 T3SS (Takaya et al., 2019), it is feasible that non-Ysc T3SSs do possess alternative mechanisms serving the same purpose as does YscX–YscY function. Presumably, specific variations have evolved among different T3SS families given the evolutionary divergence of T3SS that has occurred with respect to different host cell tropisms (Abby & Rocha, 2012).

As a tool to report on YscX secretion, YscX-Bla fusion proteins were engineered based on the experiences from a previous study by this laboratory (Amer et al., 2011). The method is convenient, but it is necessary to keep in mind a couple of caveats. Although the native β-lactamase reporter protein is stable (Amer et al., 2011), the measurable levels of accumulated β-lactamase reporter protein can be influenced by at least two factors. The first factor is the efficiency

of translation of the appended sequence at the N-terminus of the reporter protein. This is illustrated herein with the $YscX_1$-Bla and $YscX_5$-Bla fusions. Both generated stable product (see Figure S1b), but the amount of the $YscX_1$-Bla product accumulated is much lower than for the $YscX_5$-Bla (see Figure 1a). This is a clear indication that the *yscX* sequence encoding the first 5 codons translates more efficiently than does the shorter sequences of 1 codon. The second factor is the change in overall folding of recombinant Bla fusion proteins that can lead to increased susceptibility to digestion by intracellular proteases. This is exemplified by a comparison of the longer fusions $YscX_{15}$-Bla and $YscX_{20}$-Bla. Both accumulate equivalent steady-state levels, suggesting similar translation efficiencies (see Figure 1a). However, the larger $YscX_{20}$-Bla fusion is noticeably less stable, and stability deteriorates further with the appending of longer *yscX* sequences to the N-terminus of Bla (see Figure S1b). It is important to be kept in mind these caveats since they would influence any translational reporter system. Nevertheless, in our hands not only did the Ysc-Bla translational reporter fusions identify the first ten codons as a minimal N-terminal secretion signal for YscX, but they also indicated that elements of *yscX* translation control exist within the N-terminus region. This important observation will be followed up in future work, because mechanisms of translation control are under-appreciated in the T3SS research community. Furthermore, we are also keen to address why appending a tag at the YscX C-terminus has a dramatic negative impact on the integrity of the recombinant YscX. We infer from this work that the C-terminus of YscX is intolerant to genetic manipulation. Realistically, this effect can be understood only after a structure of YscX has been resolved.

Finally, one other serendipitous finding from this work concerned the loss of secretion control in the reciprocal $YscX_{2\text{-}15}$-LcrQ chimera. It was evident that in non-secretion-permissive conditions bacteria producing and secreting a variant of LcrQ that contained residues 2 to 15 derived from YscX secreted at least SctB, SctE and YopE. This is a bold phenotype and mimicking loss-of-function *lcrQ* mutants (Li et al., 2014a; Rimpiläinen et al., 1992; Stainier et al., 1997; Wulff-Strobel et al., 2002). There is little understanding of the molecular mechanism of LcrQ secretion control even in light of new findings linking LcrQ with the LcrH-YopD complex (Fei et al., 2021). Hence, the expression and secretion profile of $YscX_{2\text{-}15}$-LcrQ inevitably needs further investigation. This finding is vital, because it indicates that information in the LcrQ secretor domain impacts the regulation of T3SS activity and that having a YscX derived secretion signal may lead to premature secretion of $YscX_{2\text{-}15}$-LcrQ. Importantly, this effect is specific to LcrQ function. This will form a testable hypothesis as the basis for future work.

4 | EXPERIMENTAL PROCEDURES

4.1 | Bacterial strains and growth conditions

The bacterial strains we used in this study are listed in Table S2. Bacteria were routinely cultivated in Luria Bertani (LB) agar or broth at either 26°C (*Y. pseudotuberculosis*) or 37°C (*E. coli*) with aeration. Antibiotics were added when required at the final concentrations of Cb; 100 μg per ml (carbenicillin—Cb), 50 μg per ml (kanamycin—Km) and 25 μg per ml (chloramphenicol—Cm). Analysis of T3SS by *Y. pseudotuberculosis* occurred at 37°C in Brain heart infusion (BHI) broth. Media containing Ca^{2+} ions was the non-inducing condition (BHI supplemented with 2.5 mM $CaCl_2$), while media devoid of Ca^{2+} ions was the inducing condition (BHI supplemented with 20 mM $MgCl_2$ and 5 mM Ethylene glycol-bis-[β-aminoethyl ether]-N,N,N′,N′-tetraacetic acid).

4.2 | PCR amplification and sequence analysis

Amplified DNA fragments obtained by PCR used the appropriate oligonucleotide combination listed as online supplementary information (Table S3). Sigma-Aldrich Co (Dorset, England) synthesized these custom oligonucleotides. Amplified fragments were confirmed to be mutation free by being first cloned using the InsTAclone PCR cloning kit (Thermo Fisher Scientific, Inc.) and then sequenced by Eurofins MWG Operon AG (Ebersberg, Germany).

4.3 | Site-directed mutagenesis and allelic exchange by homologous recombination

For the construction of in-frame *yscX* deletions and chimeric variants harboring exchanged N-terminal secretor domains, mutagenized DNA fragments were generated by overlap PCR (Horton & Pease, 1991). DNA fragments were cloned into the XhoI-XbaI digested suicide mutagenesis vector, pDM4 (Milton et al., 1996). These plasmids transferred into *E. coli* S17-1λ*pir* served as the donors in conjugal matings with the appropriate *Y. pseudotuberculosis* recipients. Selection based on Cm resistance enabled the isolation of conjugates having an initial single homologous recombination event that lead to integration of the entire mutagenesis plasmid. This was followed by conventional sucrose sensitivity measures (Milton et al., 1996) to enhance selection for appropriate secondary homologous recombination events that facilitated exchange of wild type alleles with mutated alleles and concomitant mutagenesis plasmid excision. Verification of generated *in cis* mutations on the virulence plasmid utilized a combination of diagnostic PCR and sequence analysis prior to use.

4.4 | Generation of epitope-tagged protein expression constructs

yscX incorporating either a His_6 N-terminal or C-terminal epitope tag was PCR amplified and ligated into the *Pst*I and *Bam*HI sites within the pMMB208 expression vector. In addition, *yscX* and N-terminal deletions *yscX* variants with a 5-prime FLAG™ epitope were PCR amplified and cloned into *Bam*HI-*Eco*RI digested pMMB208. Similarly, *yscY* incorporating either a FLAG™

N-terminal or C-terminal epitope tag was PCR amplified and ligated into *Pst*I and *Bam*HI restricted pMMB208. This placed the epitope-tagged alleles under an IPTG inducible promoter. The constructs in *E. coli* S17-1λ*pir* were mobilized into the appropriate *Yersinia* background.

4.5 | Detection of type III substrate synthesis and secretion

Induction of type III substrate synthesis and secretion from *Y. pseudotuberculosis* was essentially performed as previously described (Amer et al., 2011). Sampled protein content was either directly from 2 ml bacterial cultures or from 10 ml culture volumes first precipitated with trichloroacetic acid. Sampling direct from the bacterial suspension, which contains a mix of protein associated with bacteria and protein released into the supernatant, assessed total protein content. Sampling of the cleared supernatant provided an assessment of the secreted protein levels. Fractionation of collected protein samples was performed by SDS–PAGE. To detect individual proteins, SDS–PAGE fractionated protein was wet transferred onto PDVF membranes and subjected to immunoblotting. Chemiluminescent detection utilized the Thermo Scientific Pierce ECL 2 Western Blotting Substrate.

4.6 | Antibodies and antibody production

Primary rabbit polyclonal antisera raised against the secreted SctE, SctB, and YopE were a gift from Hans Wolf-Watz (Umeå University, Sweden). Primary rabbit polyclonal antisera raised against the synthetic peptide (NH_2-)CLHRAQDYRRELDTL(-$CONH_2$) incorporating the residues 70 to 83 of YscX was generated by AgriSera AB (Vännäs, Sweden). Antibodies to various other Ysc antibodies were generated by Agrisera AB and were raised against the purified proteins ZZ-SctO, His-SctJ, His-SctK, His-SctN, His-SctC (residues 26 to 242), SctI and SctD (residues 143 to 419). Mikael Lindberg at the Protein Expertise Platform, Umeå University, expressed and purified all proteins. Mouse monoclonal anti-Penta-His antibody and mouse monoclonal anti-Flag M2 antibody were purchased from Qiagen GmbH (#34669; Hilden, Germany) and Sigma (#F3165; St Louis, Missouri, USA) respectively. Secondary antisera was anti-rabbit or anti-mouse antibody conjugated to horseradish peroxidase (GE Healthcare, Buckinghamshire, United Kingdom).

4.7 | Yeast plasmid construction, transformation, and n-hybrid assays

The $yscX_{\Delta 3\text{-}7}$, $yscX_{\Delta 8\text{-}12}$, and $yscX_{\Delta 13\text{-}22}$ alleles were amplified by PCR using primers described in Table S3 and translationally fused to the GAL4 activation domain in the yeast two-hybrid vector pGADT7 (Clontech Laboratories, Palo Alto, CA) (Table S2). The generation of a construct expressing the wild type *yscX* allele in pGADT7, and a construct expressing the native *yscY* allele fused to the GAL4 DNA binding domain in pGBKT7 have been described previously (Bröms et al., 2005; Francis et al., 2001). Transformation of the *S. cerevisiae* reporter strain AH109 was performed as described earlier (Francis et al., 2000). Protein interactions from multiple independent transformations were determined by measuring the activation of the *ADE2* reporter gene activation and the *HIS3* reporter gene during growth on tryptophan and leucine minus SD synthetic minimal medium also lacking either adenine or histidine, respectively. The latter also required the addition of 4 mM 3-aminotriazole in the growth media to overcome any risk of false positives (James et al., 1996).

To confirm the stable production of the bacterial proteins in yeast, we adapted a previously described protocol (Francis et al., 2000). Overnight cultures were grown in minimal selection medium. A volume of 0.1 was used to inoculate 50 ml of fresh non-selective YPD medium. Cultures were then grown at 30°C until mid-log phase (OD_{600} between 0.4 and 0.6), chilled quickly, and then harvested by centrifugation at 1000 RCF for 5 min at 4°C. Pellets were washed in equal volume ice-cold H_2O, then immediately frozen in a dry ice-ethanol bath. Cracking buffer [8 M urea, 5% (v/v) SDS, 40 mM Tris–HCl, pH 6.8, 0.1 mM EDTA, 0.4% (w/v) bromophenol blue] was prewarmed to 60°C, and a final concentration of 1% (v/v) β-mercaptoethanol, Complete protease inhibitor cocktail (Boehringer Mannheim; used at a concentration recommended by the manufacturer) and 174.2 μg/ml phenylmethylsulphonyl fluoride (PMSF) were added immediately before use. Subsequently, PMSF was added every additional ~7 min. Yeast was rapidly thawed at 60°C in 300 μl of cracking buffer and transferred directly into a 0.8 volume of glass beads contained in 2 ml reaction tubes. Samples were heated at 70°C for 10 min before a vigorous 1 min vortex. Cell debris and unbroken cells were pelleted at 4°C for 5 min at 14,000 rpm. Supernatants were collected into fresh ice-cold 2 ml reaction tubes containing PMSF. Following denaturation at 95°C for 5 min, samples were immediately fractionated by SDS–PAGE and protein content visualized by immunoblot. Proteins fused to the GAL4 DNA binding domain were detected with mouse monolclonal anti-GAL4 DNA BD antibody (#630403, Clontech Laboratories Inc). Proteins fused to the GAL4 activation domain were detected with mouse monolclonal anti-HA antibody (clone 12CA5) (Roche Diagnostics Corp.).

Yeast three-hybrid assays used pGADT7 and the pBridge vector (Clontech Laboratories). This method is assayed for specific protein–protein interactions in the context of a third protein. From the pBridge vector, YscY was constitutive expressed as a Gal4 DNA BD fusion protein through the alcohol dehydrogenase promoter (MCSI cloning site). Additionally, variants of YscX were set up to be conditionally expressed from the MET25 promoter (cloning site MCSII) that is supposed to be inactive in the presence of 1 mm methionine, and active in the absence of methionine. Moreover, a third recombinant protein, a truncate of SctV encompassing the cytoplasmic-located soluble C-terminal domain incorporating amino acids 322 to 704, was set up as a GAL4 activation domain fusion through cloning into pGADT7. The resulting vector constructs were transformed into

both *S. cerevisiae* Y190 and HF7c strains to permit dual reporter gene measurements via β-galactosidase assays (*lacZ* reporter) and growth on histidine dropout media (*HIS3* reporter), respectively.

4.8 | Construction and analysis of YscX translationally fused to signalless β-lactamase

Various length translational fusions linking the 5-prime region of *yscX*, including the predicted Shine-Dalgarno (SD) sequence, to truncated *bla* were then generated in pAA010 that contains a secretion signal less *bla* reporter under IPTG inducible control. This was achieved by *Bam*HI-*Kpn*I cloning in two ways. Larger DNA fragments (>75 base pairs) were first amplified by PCR with the appropriate primer pairings listed in Table S3 and using lysed YPIII/pIB102 as a source of template DNA. Smaller DNA fragments (<45 base pairs) were formed by the annealing of two complementary oligonucleotides prior to DNA ligation to the vector (Table S3). Analysis of recombinant β-Lactamase synthesis and secretion followed the trichloracetic acid-precipitation procedure for large-scale Yop synthesis and secretion analysis. After Western blot of fractionated protein, fusion proteins were detected with a primary mouse monoclonal anti-β-Lactamase antibody (MA1-20370, Thermo Scientific) followed by incubation with α-rabbit antiserum conjugated with horse radish peroxidase (GE Healthcare) and Pierce ECL 2 Western Blotting Substrate.

4.9 | Intrabacterial protein stability

Intrabacterial protein stability in the presence of intracellular proteases was assessed after growth in BHI (Brain Heart Infusion) medium supplemented with 2.5 mM $CaCl_2$ (BHI + Ca^{2+}) as described previously (Feldman et al., 2002). Fractionation of collected protein samples was by SDS–PAGE. For specific detection, protein was transferred onto a PDVF membrane. Membrane bound native YscX was detected with rabbit polyclonal YscX antiserum and recombinant YscX-Bla fusions with a rabbit polyclonal β-lactamase antiserum (#AB3738, Millipore), followed by horseradish peroxidase conjugated anti-rabbit antibody prior to chemiluminescent detection with the Pierce ECL 2 Western Blotting Substrate.

4.10 | SctF surface localization and chemical cross-linking

Overnight cultures from *Yersinia* strains were grown with shaking at 26°C in 2 ml of BHI broth supplemented with 2.5 mM $CaCl_2$. Subsequently, 0.1 volumes of bacterial suspension were sub-cultured into 3 ml fresh media and incubated for 3 h at 37°C. After each culture was standardized by A_{600}, 1 ml volumes were harvested by centrifugation at 8000 *g* for 5 min at 4°C. Each bacterial pellet was gently suspended in 1 ml of cold 20 mM HEPES, 2.5 mM $CaCl_2$ (pH 8). Bacterial surface proteins were cross-linked for 30 min at RT with the non-cleavable, membrane-impermeable, amine-reactive cross-linker Pierce BS^3 (Thermo Scientific) at a final concentration of 5 mM. Cross-linking reactions were quenched for 15 min by addition of Tris–HCl (pH 8.0) to a final concentration of 20 mM. Cell fractions were collected by centrifugation at 12,200 *g* for 5 min at 4°C. Bacterial pellets were then suspended in 100 μl of 1X sample buffer and analyzed by 12% acrylamide SDS–PAGE and immunoblotting with rabbit anti-SctF polyclonal antiserum (a gift from Hans Wolf-Watz) that underwent several rounds of immunoadsorption with purified SctF to enhance its monospecificity.

4.11 | Cell fractionation and Ysc component localization

Bacterial cell fractionation of *Y. pseudotuberculosis* was performed as described previously with some modifications (Filip et al., 1973; Obi et al., 2011; Vesto et al., 2018). Following induction of T3S, cells from 2 ml of bacterial culture were normalized to the amount of bacterial cells at an optical density of 600 nm. Pelleted cells were obtained by centrifugation at 6000*g* for 10 min at 4°C, washed once with 1 ml of PBS and resuspended in 1 ml of ice-cold osmotic shock buffer (30 mM Tris–Hcl, pH 8, 20% (w/v) sucrose). After addition of EDTA to a final concentration of 2.5 mM and 15 min gentle agitation at 4°C, cells were pelleted at 3000*g* for 12 min, resuspended in 300 μl of ice-cold 5 mM $MgSO_4$, and kept at ice for 20 min. The supernatant collected after centrifugation at 14,000*g* for 10 min represented the periplasmic fraction. The pellet was then resuspended in 1 ml of lysis buffer (100 mM Tris–HCl, pH 8.0, 10 mM EDTA) and lysed on ice by sonication. Intact bacteria and unbroken cells were removed by centrifugation at 14,000*g* for 5 min at 4°C. The supernatant was subjected to ultracentrifugation at 185,000*g* for 35 min at 4°C to recover cytoplasmic proteins (supernatant). The pellet (total membrane fraction) was then washed with 500 μl of 20 mM potassium phosphate buffer, pH 7.0 at 208,000*g* for 12 min. To separate inner and outer membrane proteins, the pellet was resuspended in 250 μl of 0.5% sarcosyl in 20 mM potassium phosphate buffer, pH 7.0 and incubated at room temperature for 30 min with gentle agitation. This mixture was centrifuged at 20,800*g* for 45 min at 4°C. The soluble fraction contained the inner membrane proteins. The pellet enriched in outer membrane proteins was resuspended in 250 μl of 30 mM Tris–HCl, pH 8.0. All the sub-cellular fractions were standardized to the same concentration as measured by BCA protein assay kit (Pierce). Following standardization, 200 μl of each cellular fraction was mixed with 50 μl of 4 X SDS sample buffer and analyzed by SDS/PAGE (12%–18%) and immunoblotting. To confirm the integrity of cellular fractionation, rabbit polyclonal antibodies raised against H-NS, FtsH, SurA, and OmpA were used as the cytoplasmic, inner membrane, periplasmic, and outer membrane marker respectively (Obi et al., 2011; Sal-Man et al., 2013).

4.12 | Kinetics of SctU autoproteolysis

The construction of pML13 (*sctU* appended with a 3-prime FLAG™ and cloned under the *tac* promoter of pMMB66EH) has been described previously (Lavander et al., 2002). The plasmid pML13 was conjugated into recipient *Yersinia* strains that either contained YscX variants or lacked YscX. Cultures of *Yersinia* were grown in BHI—Ca^{2+} at 26°C for 1 h. Following expression of SctU-FLAG™ with 0.4 mM IPTG, cultures were grown for an additional 1 h at 37°C. At time point 0, chloramphenicol was added to a final concentration of 50 μg/ml to the bacterial culture to inhibit *de novo* protein synthesis. Thereafter, bacterial cultures were collected at indicated time points and normalized to the number of bacterial cells at an optical density of 600 nm. Protein samples associated with bacterial pellets were then suspended in 1 X SDS sample buffer to be analyzed by SDS–PAGE and immunoblotted with mouse monoclonal anti-Flag M2 antibody.

ACKNOWLEDGMENTS

We acknowledge Anton Zavialov for valuable discussion surrounding YscX and YscY function. Mikael Lindberg and the Protein Expertise Platform at Umeå University is acknowledged for successful efforts to express and purify proteins for antibody production. We also express gratitude to Hans Wolf-Watz for the gift of parental *Y. pseudotuberculosis* and antiserum against SctF, YopE, SctB, and SctE, as well as Debra Milton for the gift of pDM4, and Eckardt Treuter for the yeast strain HF7c. The authors thank also Viktor Skog for performing a linguistic review of the manuscript. Performed within the framework of the Umeå Centre for Microbial Research, support for this work was through grants from the Swedish Research Council (MSF; grant numbers: 2014-2105 and 2018-02676), Foundation for Medical Research at Umeå University (MSF), and J. C. Kempe Memorial Fund (JMG and AAA). SC acknowledges financial support from National Natural Science Foundation of China (grant number: 31570132) and recognises support from the Core Facility and Technical Support, Wuhan Institute of Virology. AD acknowledges financial support from the Max Planck Society.

CONFLICT OF INTEREST

The authors declare that the research was conducted in the absence of any commercial or financial relationships that could be construed as a potential conflict of interest.

AUTHOR CONTRIBUTIONS

Conceived and designed the experiments: JMG, AAA, AD, MSF. Provided critical reagents: SC. Performed the experiments: JMG, AAA, AD. Analyzed the data: JMG, AAA, SC, AD, MSF. Wrote the paper: JMG, MSF. All authors read and approved the paper.

DATA AVAILABILITY STATEMENT

The raw data supporting the conclusions of this article will be made available by the authors, without undue reservation.

ORCID

Shiyun Chen https://orcid.org/0000-0002-6224-2975
Andreas Diepold https://orcid.org/0000-0002-4475-3923
Matthew S. Francis https://orcid.org/0000-0001-6817-9535

REFERENCES

Abby, S.S. & Rocha, E.P. (2012) The non-flagellar type III secretion system evolved from the bacterial flagellum and diversified into host-cell adapted systems. *PLoS Genetics*, *8*, e1002983.

Altschul, S.F., Madden, T.L., Schaffer, A.A., Zhang, J., Zhang, Z., Miller, W. et al. (1997) Gapped BLAST and PSI-BLAST: a new generation of protein database search programs. *Nucleic Acids Research*, *25*, 3389–3402.

Altschul, S.F., Wootton, J.C., Gertz, E.M., Agarwala, R., Morgulis, A., Schaffer, A.A. et al. (2005) Protein database searches using compositionally adjusted substitution matrices. *The FEBS Journal*, *272*, 5101–5109.

Amer, A.A., Ahlund, M.K., Broms, J.E., Forsberg, A. & Francis, M.S. (2011) Impact of the N-terminal secretor domain on YopD translocator function in *Yersinia pseudotuberculosis* type III secretion. *Journal of Bacteriology*, *193*, 6683–6700.

Bittner, L.M., Arends, J. & Narberhaus, F. (2017) When, how and why? Regulated proteolysis by the essential FtsH protease in *Escherichia coli*. *Biological Chemistry*, *398*, 625–635.

Bjornfot, A.C., Lavander, M., Forsberg, A. & Wolf-Watz, H. (2009) Autoproteolysis of YscU of *Yersinia pseudotuberculosis* is important for regulation of expression and secretion of Yop proteins. *Journal of Bacteriology*, *191*, 4259–4267.

Blaylock, B., Riordan, K.E., Missiakas, D.M. & Schneewind, O. (2006) Characterization of the *Yersinia enterocolitica* type III secretion ATPase YscN and its regulator, YscL. *Journal of Bacteriology*, *188*, 3525–3534.

Blocker, A., Jouihri, N., Larquet, E., Gounon, P., Ebel, F., Parsot, C. et al. (2001) Structure and composition of the *Shigella flexneri* "needle complex", a part of its type III secreton. *Molecular Microbiology*, *39*, 652–663.

Bröms, J.E., Edqvist, P.J., Carlsson, K.E., Forsberg, Å. & Francis, M.S. (2005) Mapping of a YscY binding domain within the LcrH chaperone that is required for regulation of *Yersinia* type III secretion. *Journal of Bacteriology*, *187*, 7738–7752.

Broz, P., Mueller, C.A., Muller, S.A., Philippsen, A., Sorg, I., Engel, A. et al. (2007) Function and molecular architecture of the *Yersinia* injectisome tip complex. *Molecular Microbiology*, *65*, 1311–1320.

Burghout, P., van Boxtel, R., Van Gelder, P., Ringler, P., Muller, S.A., Tommassen, J. et al. (2004) Structure and electrophysiological properties of the YscC secretin from the type III secretion system of *Yersinia enterocolitica*. *Journal of Bacteriology*, *186*, 4645–4654.

Butan, C., Lara-Tejero, M., Li, W., Liu, J. & Galan, J.E. (2019) High-resolution view of the type III secretion export apparatus in situ reveals membrane remodeling and a secretion pathway. *Proceedings of the National Academy of Sciences of the United States of America*, *116*, 24786–24795.

Cao, S.Y., Liu, W.B., Tan, Y.F., Yang, H.Y., Zhang, T.T., Wang, T. et al. (2017) An interaction between the inner rod protein YscI and the needle protein YscF is required to assemble the needle structure of the *Yersinia* type three secretion system. *The Journal of Biological Chemistry*, *292*, 5488–5498.

Confer, A.W. & Ayalew, S. (2013) The OmpA family of proteins: roles in bacterial pathogenesis and immunity. *Veterinary Microbiology*, *163*, 207–222.

Cornelis, G.R., Boland, A., Boyd, A.P., Geuijen, C., Iriarte, M., Neyt, C. et al. (1998) The virulence plasmid of *Yersinia*, an antihost genome. *Microbiology and Molecular Biology Reviews*, *62*, 1315–1352.

Day, J.B. & Plano, G.V. (2000) The *Yersinia* pestis YscY protein directly binds YscX, a secreted component of the type III secretion machinery. *Journal of Bacteriology*, *182*, 1834–1843.

Dewoody, R.S., Merritt, P.M. & Marketon, M.M. (2013) Regulation of the *Yersinia* type III secretion system: traffic control. *Frontiers in Cellular and Infection Microbiology*, *3*, 4.

Diepold, A., Amstutz, M., Abel, S., Sorg, I., Jenal, U. & Cornelis, G.R. (2010) Deciphering the assembly of the *Yersinia* type III secretion injectisome. *The EMBO Journal*, *29*, 1928–1940.

Diepold, A., Kudryashev, M., Delalez, N.J., Berry, R.M. & Armitage, J.P. (2015) Composition, formation, and regulation of the cytosolic c-ring, a dynamic component of the type III secretion injectisome. *PLoS Biology*, *13*, e1002039.

Diepold, A. & Wagner, S. (2014) Assembly of the bacterial type III secretion machinery. *FEMS Microbiology Reviews*, *38*, 802–822.

Diepold, A., Wiesand, U., Amstutz, M. & Cornelis, G.R. (2012) Assembly of the *Yersinia* injectisome: the missing pieces. *Molecular Microbiology*, *85*, 878–892.

Diepold, A., Wiesand, U. & Cornelis, G.R. (2011) The assembly of the export apparatus (YscR,S,T,U,V) of the *Yersinia* type III secretion apparatus occurs independently of other structural components and involves the formation of an YscV oligomer. *Molecular Microbiology*, *82*, 502–514.

Dohlich, K., Zumsteg, A.B., Goosmann, C. & Kolbe, M. (2014) A substrate-fusion protein is trapped inside the Type III secretion system channel in *Shigella flexneri*. *PLoS Pathogens*, *10*, e1003881.

Duchaud, E., Rusniok, C., Frangeul, L., Buchrieser, C., Givaudan, A., Taourit, S. et al. (2003) The genome sequence of the entomopathogenic bacterium *Photorhabdus luminescens*. *Nature Biotechnology*, *21*, 1307–1313.

Erhardt, M., Wheatley, P., Kim, E.A., Hirano, T., Zhang, Y., Sarkar, M.K. et al. (2017) Mechanism of type-III protein secretion: regulation of FlhA conformation by a functionally critical charged-residue cluster. *Molecular Microbiology*, *104*, 234–249.

Fabiani, F.D., Renault, T.T., Peters, B., Dietsche, T., Galvez, E.J.C., Guse, A. et al. (2017) A flagellum-specific chaperone facilitates assembly of the core type III export apparatus of the bacterial flagellum. *PLoS Biology*, *15*, e2002267.

Fei, K., Yan, H., Zeng, X., Huang, S., Tang, W., Francis, M.S. et al. (2021) LcrQ coordinates with the YopD-LcrH complex to repress lcrF expression and control type III secretion by *Yersinia pseudotuberculosis*. *mBio*, *12*, e0145721.

Feldman, M.F., Muller, S., Wuest, E. & Cornelis, G.R. (2002) SycE allows secretion of YopE-DHFR hybrids by the *Yersinia enterocolitica* type III Ysc system. *Molecular Microbiology*, *46*, 1183–1197.

Filip, C., Fletcher, G., Wulff, J.L. & Earhart, C.F. (1973) Solubilization of the cytoplasmic membrane of *Escherichia coli* by the ionic detergent sodium-lauryl sarcosinate. *Journal of Bacteriology*, *115*, 717–722.

Francis, M.S. (2010) Type III secretion chaperones: a molecular toolkit for all occasions. In: Durante, P. & Colucci, L. (Eds.) *Handbook of molecular chaperones: roles, structures and mechanisms*. Hauppauge, New York: Nova Science Publishers, Inc, pp. 79–147.

Francis, M.S., Aili, M., Wiklund, M.L. & Wolf-Watz, H. (2000) A study of the YopD-LcrH interaction from *Yersinia pseudotuberculosis* reveals a role for hydrophobic residues within the amphipathic domain of YopD. *Molecular Microbiology*, *38*, 85–102.

Francis, M.S., Lloyd, S.A. & Wolf-Watz, H. (2001) The type III secretion chaperone LcrH co-operates with YopD to establish a negative, regulatory loop for control of Yop synthesis in *Yersinia pseudotuberculosis*. *Molecular Microbiology*, *42*, 1075–1093.

Frost, S., Ho, O., Login, F.H., Weise, C.F., Wolf-Watz, H. & Wolf-Watz, M. (2012) Autoproteolysis and intramolecular dissociation of *Yersinia* YscU precedes secretion of its C-terminal polypeptide YscU(CC). *PLoS One*, *7*, e49349.

Gauthier, A. & Finlay, B.B. (2003) Translocated intimin receptor and its chaperone interact with ATPase of the type III secretion apparatus of enteropathogenic *Escherichia coli*. *Journal of Bacteriology*, *185*, 6747–6755.

Gazi, A.D., Sarris, P.F., Fadouloglou, V.E., Charova, S.N., Mathioudakis, N., Panopoulos, N.J. et al. (2012) Phylogenetic analysis of a gene cluster encoding an additional, rhizobial-like type III secretion system that is narrowly distributed among *Pseudomonas syringae* strains. *BMC Microbiology*, *12*, 188.

Ginocchio, C.C. & Galán, J.E. (1995) Functional conservation among members of the *Salmonella typhimurium* InvA family of proteins. *Infection and Immunity*, *63*, 729–732.

Grabowski, B., Schmidt, M.A. & Ruter, C. (2017) Immunomodulatory *Yersinia* outer proteins (Yops)-useful tools for bacteria and humans alike. *Virulence*, *8*, 1124–1147.

Grainger, D.C. (2016) Structure and function of bacterial H-NS protein. *Biochemical Society Transactions*, *44*, 1561–1569.

Gurung, J.M., Amer, A.A., Francis, M.K., Costa, T.R., Chen, S., Zavialov, A.V. et al. (2018) Heterologous complementation studies with the YscX and YscY protein families reveals a specificity for *Yersinia pseudotuberculosis* type III secretion. *Frontiers in Cellular and Infection Microbiology*, *8*, 80.

Ho, O., Rogne, P., Edgren, T., Wolf-Watz, H., Login, F.H. & Wolf-Watz, M. (2017) Characterization of the ruler protein interaction interface on the substrate specificity switch protein in the *Yersinia* type III secretion system. *The Journal of Biological Chemistry*, *292*, 3299–3311.

Horton, R.M. & Pease, L.R. (1991) Recombination and mutagenesis of DNA sequences using PCR. In: McPherson, M.J. (Ed.) *Directed mutagenesis: a practical approach*. New York: Oxford University Press, pp. 217–247.

Hu, B., Lara-Tejero, M., Kong, Q., Galan, J.E. & Liu, J. (2017) In situ molecular architecture of the Salmonella type III secretion machine. *Cell*, *168*, 1065–1074 e1010.

Hu, J., Worrall, L.J., Hong, C., Vuckovic, M., Atkinson, C.E., Caveney, N. et al. (2018) Cryo-EM analysis of the T3S injectisome reveals the structure of the needle and open secretin. *Nature Communications*, *9*, 3840.

Hu, J., Worrall, L.J., Vuckovic, M., Hong, C., Deng, W., Atkinson, C.E. et al. (2019) T3S injectisome needle complex structures in four distinct states reveal the basis of membrane coupling and assembly. *Nature Microbiology*, *4*, 2010–2019.

Iriarte, M. & Cornelis, G.R. (1999) Identification of SycN, YscX, and YscY, three new elements of the *Yersinia* yop virulon. *Journal of Bacteriology*, *181*, 675–680.

James, P., Halladay, J. & Craig, E.A. (1996) Genomic libraries and a host strain designed for highly efficient two-hybrid selection in yeast. *Genetics*, *144*, 1425–1436.

Johnson, S., Kuhlen, L., Deme, J.C., Abrusci, P. & Lea, S.M. (2019) The structure of an injectisome export gate demonstrates conservation of architecture in the core export gate between flagellar and virulence type III secretion systems. *mBio*, *10*, e00818-19.

Kato, J., Dey, S., Soto, J.E., Butan, C., Wilkinson, M.C., De Guzman, R.N. et al. (2018) A protein secreted by the Salmonella type III secretion system controls needle filament assembly. *eLife*, *7*, e35886.

Kimbrough, T.G. & Miller, S.I. (2000) Contribution of *Salmonella typhimurium* type III secretion components to needle complex formation. *Proceedings of the National Academy of Sciences of the United States of America*, *97*, 11008–11013.

Kimbrough, T.G. & Miller, S.I. (2002) Assembly of the type III secretion needle complex of *Salmonella typhimurium*. *Microbes and Infection*, *4*, 75–82.

Koster, M., Bitter, W., de Cock, H., Allaoui, A., Cornelis, G.R. & Tommassen, J. (1997) The outer membrane component, YscC, of the Yop secretion machinery of *Yersinia enterocolitica* forms a ring-shaped multimeric complex. *Molecular Microbiology*, *26*, 789–797.

Kubori, T., Sukhan, A., Aizawa, S.I. & Galán, J.E. (2000) Molecular characterization and assembly of the needle complex of the *Salmonella typhimurium* type III protein secretion system. *Proceedings of the National Academy of Sciences of the United States of America*, *97*, 10225–10230.

Kuhlen, L., Johnson, S., Cao, J., Deme, J.C. & Lea, S.M. (2021) Nonameric structures of the cytoplasmic domain of FlhA and SctV in the context of the full-length protein. *PLoS One*, *16*, e0252800.

Lara-Tejero, M., Kato, J., Wagner, S., Liu, X. & Galan, J.E. (2011) A sorting platform determines the order of protein secretion in bacterial type III systems. *Science*, *331*, 1188–1191.

Lavander, M., Sundberg, L., Edqvist, P.J., Lloyd, S.A., Wolf-Watz, H. & Forsberg, Å. (2002) Proteolytic cleavage of the FlhB homologue YscU of *Yersinia pseudotuberculosis* is essential for bacterial survival but not for type III secretion. *Journal of Bacteriology*, *184*, 4500–4509.

Li, L., Yan, H., Feng, L., Li, Y., Lu, P., Hu, Y. et al. (2014a) LcrQ blocks the role of LcrF in regulating the Ysc-Yop type III secretion genes in *Yersinia pseudotuberculosis*. *PLoS One*, *9*, e92243.

Li, Y., Li, L., Huang, L., Francis, M.S., Hu, Y. & Chen, S. (2014b) *Yersinia* Ysc-Yop type III secretion feedback inhibition is relieved through YscV-dependent recognition and secretion of LcrQ. *Molecular Microbiology*, *91*, 494–507.

Lountos, G.T., Tropea, J.E. & Waugh, D.S. (2012) Structure of the cytoplasmic domain of *Yersinia* pestis YscD, an essential component of the type III secretion system. *Acta Crystallographica Section D, Biological Crystallography*, *68*, 201–209.

Löwer, M. & Schneider, G. (2009) Prediction of type III secretion signals in genomes of gram-negative bacteria. *PLoS One*, *4*, e5917.

Mahdavi, A., Szychowski, J., Ngo, J.T., Sweredoski, M.J., Graham, R.L., Hess, S. et al. (2014) Identification of secreted bacterial proteins by noncanonical amino acid tagging. *Proceedings of the National Academy of Sciences of the United States of America*, *111*, 433–438.

Majewski, D.D., Lyons, B.J.E., Atkinson, C.E. & Strynadka, N.C.J. (2020) Cryo-EM analysis of the SctV cytosolic domain from the enteropathogenic *E. coli* T3SS injectisome. *Journal of Structural Biology*, *212*, 107660.

Marlovits, T.C., Kubori, T., Lara-Tejero, M., Thomas, D., Unger, V.M. & Galan, J.E. (2006) Assembly of the inner rod determines needle length in the type III secretion injectisome. *Nature*, *441*, 637–640.

Mas, G., Thoma, J. & Hiller, S. (2019) The periplasmic chaperones Skp and SurA. *Sub-Cellular Biochemistry*, *92*, 169–186.

Mattei, P.J., Faudry, E., Job, V., Izore, T., Attree, I. & Dessen, A. (2011) Membrane targeting and pore formation by the type III secretion system translocon. *The FEBS Journal*, *278*, 414–426.

Matthews-Palmer, T.R.S., Gonzalez-Rodriguez, N., Calcraft, T., Lagercrantz, S., Zachs, T., Yu, X.J. et al. (2021) Structure of the cytoplasmic domain of SctV (SsaV) from the Salmonella SPI-2 injectisome and implications for a pH sensing mechanism. *Journal of Structural Biology*, *213*, 107729.

McDermott, J.E., Corrigan, A., Peterson, E., Oehmen, C., Niemann, G., Cambronne, E.D. et al. (2011) Computational prediction of type III and IV secreted effectors in gram-negative bacteria. *Infection and Immunity*, *79*, 23–32.

Milton, D.L., O'Toole, R., Horstedt, P. & Wolf-Watz, H. (1996) Flagellin A is essential for the virulence of Vibrio anguillarum. *Journal of Bacteriology*, *178*, 1310–1319.

Mukerjea, R. & Ghosh, P. (2013) Functionally essential interaction between *Yersinia* YscO and the T3S4 domain of YscP. *Journal of Bacteriology*, *195*, 4631–4638.

Nauth, T., Huschka, F., Schweizer, M., Bosse, J.B., Diepold, A., Failla, A.V. et al. (2018) Visualization of translocons in *Yersinia* type III protein secretion machines during host cell infection. *PLoS Pathogens*, *14*, e1007527.

Obi, I.R., Nordfelth, R. & Francis, M.S. (2011) Varying dependency of periplasmic peptidylprolyl cis-trans isomerases in promoting *Yersinia pseudotuberculosis* stress tolerance and pathogenicity. *The Biochemical Journal*, *439*, 321–332.

Ogino, T., Ohno, R., Sekiya, K., Kuwae, A., Matsuzawa, T., Nonaka, T. et al. (2006) Assembly of the type III secretion apparatus of enteropathogenic *Escherichia coli*. *Journal of Bacteriology*, *188*, 2801–2811.

Osborne, S.E. & Coombes, B.K. (2011) Expression and secretion hierarchy in the nonflagellar type III secretion system. *Future Microbiology*, *6*, 193–202.

Pallen, M.J., Francis, M.S. & Futterer, K. (2003) Tetratricopeptide-like repeats in type-III-secretion chaperones and regulators. *FEMS Microbiology Letters*, *223*, 53–60.

Park, D., Lara-Tejero, M., Waxham, M.N., Li, W., Hu, B., Galan, J.E. et al. (2018) Visualization of the type III secretion mediated Salmonella-host cell interface using cryo-electron tomography. *eLife*, *7*, e39514.

Pettersson, J., Nordfelth, R., Dubinina, E., Bergman, T., Gustafsson, M., Magnusson, K.E. et al. (1996) Modulation of virulence factor expression by pathogen target cell contact. *Science*, *273*, 1231–1233.

Pha, K. & Navarro, L. (2016) *Yersinia* type III effectors perturb host innate immune responses. *World Journal of Biological Chemistry*, *7*, 1–13.

Philip, N.H., Zwack, E.E. & Brodsky, I.E. (2016) Activation and Evasion of Inflammasomes by *Yersinia*. *Current Topics in Microbiology and Immunology*, *397*, 69–90.

Radics, J., Konigsmaier, L. & Marlovits, T.C. (2014) Structure of a pathogenic type 3 secretion system in action. *Nature Structural & Molecular Biology*, *21*, 82–87.

Rimpiläinen, M., Forsberg, Å. & Wolf-Watz, H. (1992) A novel protein, LcrQ, involved in the low-calcium response of *Yersinia pseudotuberculosis* shows extensive homology to YopH. *Journal of Bacteriology*, *174*, 3355–3363.

Russo, B.C., Duncan, J.K., Wiscovitch, A.L., Hachey, A.C. & Goldberg, M.B. (2019) Activation of *Shigella flexneri* type 3 secretion requires a host-induced conformational change to the translocon pore. *PLoS Pathogens*, *15*, e1007928.

Sal-Man, N., Setiaputra, D., Scholz, R., Deng, W., Yu, A.C., Strynadka, N.C. et al. (2013) EscE and EscG are cochaperones for the type III needle protein EscF of enteropathogenic *Escherichia coli*. *Journal of Bacteriology*, *195*, 2481–2489.

Silva-Herzog, E., Ferracci, F., Jackson, M.W., Joseph, S.S. & Plano, G.V. (2008) Membrane localization and topology of the *Yersinia* pestis YscJ lipoprotein. *Microbiology*, *154*, 593–607.

Sorg, I., Wagner, S., Amstutz, M., Muller, S.A., Broz, P., Lussi, Y. et al. (2007) YscU recognizes translocators as export substrates of the *Yersinia* injectisome. *The EMBO Journal*, *26*, 3015–3024.

Soto, E., Espinosa, N., Diaz-Guerrero, M., Gaytan, M.O., Puente, J.L. & Gonzalez-Pedrajo, B. (2017) Functional characterization of EscK (Orf4), a sorting platform component of the enteropathogenic *Escherichia coli* injectisome. *Journal of Bacteriology*, *199*, e00538-16.

Stainier, I., Iriarte, M. & Cornelis, G.R. (1997) YscM1 and YscM2, two *Yersinia enterocolitica* proteins causing downregulation of yop transcription. *Molecular Microbiology*, *26*, 833–843.

Takaya, A., Takeda, H., Tashiro, S., Kawashima, H. & Yamamoto, T. (2019) Chaperone-mediated secretion switching from early to middle substrates in the type III secretion system encoded by Salmonella pathogenicity island 2. *The Journal of Biological Chemistry*, *294*, 3783–3793.

Thorslund, S.E., Edgren, T., Pettersson, J., Nordfelth, R., Sellin, M.E., Ivanova, E. et al. (2011) The RACK1 signaling scaffold protein selectively interacts with *Yersinia pseudotuberculosis* virulence function. *PLoS One*, *6*, e16784.

Torres-Vargas, C.E., Kronenberger, T., Roos, N., Dietsche, T., Poso, A. & Wagner, S. (2019) The inner rod of virulence-associated type III secretion systems constitutes a needle adapter of one helical turn that is deeply integrated into the system's export apparatus. *Molecular Microbiology*, *112*, 918–931.

Vesto, K., Huseby, D.L., Snygg, I., Wang, H., Hughes, D. & Rhen, M. (2018) Muramyl endopeptidase Spr contributes to intrinsic vancomycin

resistance in *Salmonella enterica* Serovar Typhimurium. *Frontiers in Microbiology*, *9*, 2941.

Wagner, S., Grin, I., Malmsheimer, S., Singh, N., Torres-Vargas, C.E. & Westerhausen, S. (2018) Bacterial type III secretion systems: a complex device for the delivery of bacterial effector proteins into eukaryotic host cells. *FEMS Microbiology Letters*, *365*, 1–13.

Wagner, S., Konigsmaier, L., Lara-Tejero, M., Lefebre, M., Marlovits, T.C. & Galan, J.E. (2010) Organization and coordinated assembly of the type III secretion export apparatus. *Proceedings of the National Academy of Sciences of the United States of America*, *107*, 17745–17750.

Wang, Y., Sun, M., Bao, H., Zhang, Q. & Guo, D. (2013) Effective identification of bacterial type III secretion signals using joint element features. *PLoS One*, *8*, e59754.

Wood, S.E., Jin, J. & Lloyd, S.A. (2008) YscP and YscU switch the substrate specificity of the *Yersinia* type III secretion system by regulating export of the inner rod protein YscI. *Journal of Bacteriology*, *190*, 4252–4262.

Wulff-Strobel, C.R., Williams, A.W. & Straley, S.C. (2002) LcrQ and SycH function together at the Ysc type III secretion system in *Yersinia* pestis to impose a hierarchy of secretion. *Molecular Microbiology*, *43*, 411–423.

Xing, Q., Shi, K., Portaliou, A., Rossi, P., Economou, A. & Kalodimos, C.G. (2018) Structures of chaperone-substrate complexes docked onto the export gate in a type III secretion system. *Nature Communications*, *9*, 1773.

Yang, H., Shan, Z., Kim, J., Wu, W., Lian, W., Zeng, L. et al. (2007) Regulatory role of PopN and its interacting partners in type III secretion of *Pseudomonas aeruginosa*. *Journal of Bacteriology*, *189*, 2599–2609.

Yuan, B., Portaliou, A.G., Parakra, R., Smit, J.H., Wald, J., Li, Y. et al. (2021) Structural dynamics of the functional nonameric type III translocase export gate. *Journal of Molecular Biology*, *433*, 167188.

Zhang, Y., Lara-Tejero, M., Bewersdorf, J. & Galan, J.E. (2017) Visualization and characterization of individual type III protein secretion machines in live bacteria. *Proceedings of the National Academy of Sciences of the United States of America*, *114*, 6098–6103.

Zilkenat, S., Franz-Wachtel, M., Stierhof, Y.D., Galan, J.E., Macek, B. & Wagner, S. (2016) Determination of the stoichiometry of the complete bacterial type III secretion needle complex using a combined quantitative proteomic approach. *Molecular & Cellular Proteomics*, *15*, 1598–1609.

SUPPORTING INFORMATION

Additional supporting information may be found in the online version of the article at the publisher's website.

How to cite this article: Gurung, J. M., Amer, A. A., Chen, S., Diepold, A., & Francis, M. S. (2022). Type III secretion by *Yersinia pseudotuberculosis* is reliant upon an authentic N-terminal YscX secretor domain. *Molecular Microbiology*, *117*, 886–906. https://doi.org/10.1111/mmi.14880